Multiscale structural analysis in the subducted continental crust of the internal Sesia-Lanzo Zone (Monte Mucrone, Western Alps)

Francesco Delleani, M. Iole Spalla, Daniele Castelli, Guido Gosso

Multiscale structural analysis in the subducted continental crust of the internal Sesia-Lanzo Zone (Monte Mucrone, Western Alps)

Francesco Delleani

Dipartimento di Scienze della Terra "A. Desio", Università degli Studi di Milano, Via Mangiagalli 34, 20133, Milano, Italy. *Email: francesco.delleani@unimi.it*

M. Iole Spalla

1. Dipartimento di Scienze della Terra "A. Desio", Università degli Studi di Milano, Via Mangiagalli 34, 20133, Milano, Italy
2. C.N.R.-I.D.P.A., Sezione di Milano, Via Mangiagalli 34, 20133, Milano, Italy. *Email: iole.spalla@unimi.it*

Daniele Castelli

Dipartimento di Scienze della Terra, Università degli Studi di Torino, Via Valperga Caluso 35, 10125, Torino, Italy

Guido Gosso

1. Dipartimento di Scienze della Terra "A. Desio", Università degli Studi di Milano, Via Mangiagalli 34, 20133, Milano, Italy
2. C.N.R.-I.D.P.A., Sezione di Milano, Via Mangiagalli 34, 20133, Milano, Italy

Abstract: Intrusives of Permian age and their high-grade country rocks, subducted and exhumed in Alpine time, have been studied with petro-structural high resolution mapping. In this subduction environment of the Sesia-Lanzo Zone of the internal Western Alps, focus was oriented on interaction mechanisms between deformation and progress of metamorphic transformations, in an area offering a mosaic of different tectonometamorphic evolutionary steps. Such apparently incoherent distribution of structural imprints, representing various discrete states of the tectonic sequence heterogeneously frozen in adjacent spaces, has been previously recomposed into a coherent progression of deformation events by means of foliation trajectory mapping. This work guaranteed a petrographic analysis of the mineralogical support of sequentially ordered planar fabrics. Six deformation episodes (D1 to D6) were recognised, as superposed folds, foliations and ductile shear zones systems, evidently related to the Alpine tectonic history. Petrologic estimates on time-related microstructures well manifest that eclogite facies metamorphic conditions assisted D1 and D2 deformation stages, the blueschist-facies re-equilibration was contemporaneous with D3 and the greenschist-facies re-equilibration with D4. Recognition of numerous assemblages and textures of pre-Alpine protoliths supported validity of the individuation of the earliest, more cryptic tectonic environment of the widespread eclogitisation that predates D2. The coherent correlation between structural and metamorphic mineral growth histories on a wide area served as a base for further refinement and revealed that full granular scale diffusion of newly-forming parageneses is generally related to attainment of a threshold of intensity in the development of the new planar fabrics, as similarly established in another subducted-exhumed metamorphic complex of the internal Central Alps.

Introduction

Multi-scale structural and petrographic analysis allows reconstructions, in the crustal rocks, of the tectonic evolution of orogenic belts, giving insights on the development of deformation events and the evolution of thermal history through time (e.g. Spalla *et al.*, 2000; Spalla *et al.*, 2011; Spalla *et al.*, 2005). The reconstruction of structural and metamorphic evolutions in polycyclic metamorphic terrains is performed since long time through a multidisciplinary approach based on detailed correlation of superposed fabric elements, microstructural analysis and recognition of fabric gradients (Hobbs *et al.*, 1976; Johnson & Vernon, 1995; Park, 1969; Passchier *et al.*, 1990; Salvi *et al.*, 2010; Spalla, 1993; Spalla *et al.*, 2000; Turner & Weiss, 1963; Williams, 1985; Zucali, 2002).

Rocks belonging to a single tectono-metamorphic unit generally record heterogeneously the succession of tectonic imprints and the related metamorphic re-equilibrations: in many cases this has been interpreted as due to the catalyzing effect of deformation on metamorphic reaction progress (see Hobbs *et al.*, 2010 and refs therein). At the end of the deformation history, the result is a patchy distribution of different fabrics and their supporting mineral assemblages; estimate of differently re-equilibrated volumes has given fundamental insights into the accomplishment of structural and/or metamorphic re-equilibrations at different structural levels, along active plate margins (e.g.: Salvi *et al.*, 2010; Spalla *et al.*, 2005). Such kind of evaluation could highlight, for example, the influence of different deformation mechanisms, phase transitions and, consequently, density and viscosity variations affecting the mechanical behaviour of the lithosphere in subduction zones: all these parameters play a fundamental role in quantitative geodynamic modelling. The Sesia-Lanzo Zone, which was deformed at high pressure under a very-low thermal regime in the Alpine time, represents an interesting subject to infer the deformation-metamorphism interactions in the continental crust during subduction (Roda *et al.*, 2012; Zucali & Spalla, 2011). In this paper, we infer the deformation-metamorphism relationships in the Mt. Mucrone area, where Permian intrusives are exposed with their country rocks, both belonging to the Eclogitic Micaschists Complex, to evaluate the degree of fabric evolution during successive deformation stages together with the progress of syn-kinematic metamorphic reactions. Maps were performed to detail the heterogeneous distribution of textural and metamorphic transformations, taking into account the degree of mechanical and mineral–chemical transformation of different rocks at micro- to km-scale. In these maps, low- and high-strain domains are represented for each deformation phase, and supported by information on the volumes occupied by newly formed, or relict, mineral assemblages. These maps (maps of deformation partitioning and metamorphic imprints) may facilitate the perception of the influence that the heterogeneous distribution of deformation and metamorphism can play on the lithostratigraphy variations during a polyphase tectonic evolution.

Geological setting

The Sesia-Lanzo Zone (SLZ, Fig. 1) represents the widest portion of continental crust in the Western Alps that underwent high pressure (HP) metamorphism during the Alpine subduction (e.g. Babist *et al.*, 2006; Compagnoni *et al.*, 1977; Dal Piaz *et al.*, 1972; Meda *et al.*, 2010; Pognante, 1991; Roda *et al.*, 2012), preceding the collision between European and Adria continental plates.

The Alpine metamorphic history of the SLZ comprises the record of an eclogite-facies imprint followed by blueschist- and greenschist-facies re-equilibrations (e.g. Castelli & Rubatto, 2002; Compagnoni, 1977; Gosso, 1977; Lardeaux *et al.*, 1982; Pognante, 1989a; Rebay & Messiga, 2007; Spalla *et al.*, 1983; Zucali & Spalla, 2011). Mineral ages ranging between 90 and 65 have been related to the Alpine eclogite-facies peak (Cenki-Tok *et al.*, 2011; Rubatto *et al.*, 1999). The very low T/P ratio characterising this evolution assists the preservation of many pre-Alpine igneous and metamorphic relicts in rocks with an Alpine polyphasic recrystallization. P-T conditions for the early-Alpine HP imprints range between 500–625 °C and 1.3–2.5 GPa (see Roda *et al.*, 2012 for a review of available PT estimates). The external margin of the SLZ is bounded by eclogitized ophiolitic relicts of the Liguria-Piedmont Ocean, the Piedmont Zone, and its internal margin is a thick mylonitic belt (the Canavese Line), separating SLZ from the lower crustal rocks of the Southalpine Ivrea Zone, which escaped the Alpine HP evolution (Bigi *et al.*, 1990).

Figure 1. Tectonic sketch of Western Alps (modified after Dal Piaz, 1999) showing the location of the Sesia-Lanzo Zone (SL); red diamond locates the mapped area of Fig 2.
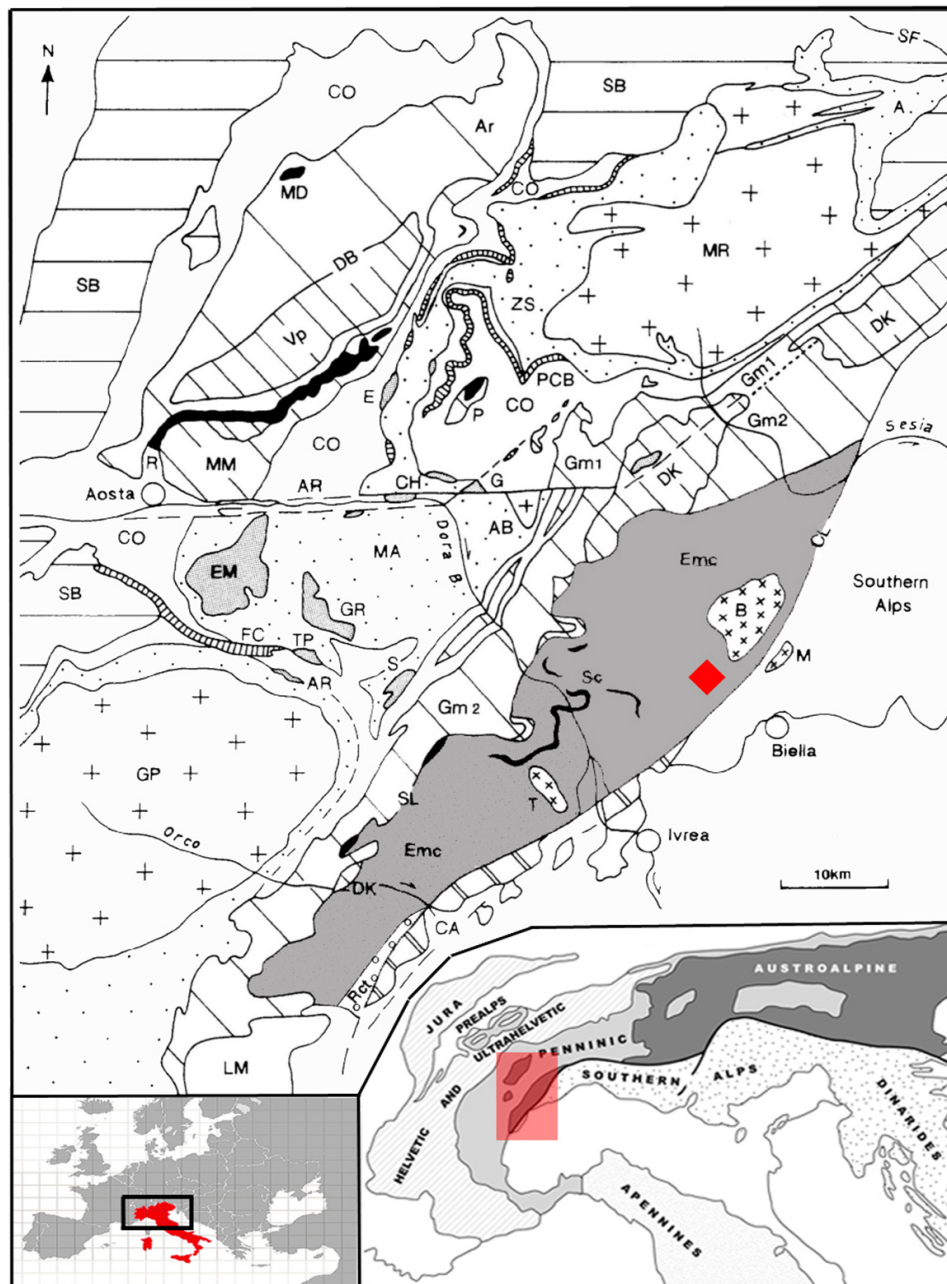
The two bottom insets locate the tectonic sketch in the frame of the European Alps. Legend: 1) Penninic continental nappes: MR = Monte Rosa, AB = Arcesa-Brusson, GP = Gran Paradiso, SB = Grand St. Bernard; 2a) Austroalpine nappes: DB = Dent Blanche (Vp = Valpelline lower crust, Ar = Arolla series), MM - P = Mt. Mary-Pillonet thrust system, AR = Acque Rosse, CH = Chatillon-St. Vincent, E = Etirol-Levaz, G = Grun, EM = Mt. Emilius, GR = Glacier-rafray, S = Santanel, TP = Tour Ponton, SL = Sesia-Lanzo Zone (Dk = Dioritic-kinzigitic upper element, Gm = Gneiss Minuti complex with (2) or without (1) eclogitic relics, Emc = Eclogitic Micaschists complex, Rct = Rocca Canavese Thrust Sheets); 2b) Mesozoic metasedimentary covers in Austroalpine Domain: R = Roisan Zone, Sc = Scalaro unit; 3) Ophiolitic Piedmont Zone: CO = Combin Zone, PCB = Pancherot-Cime Bianche, FC = Faisceau de Cogne, ZS = Zermatt-Saas Zone, MA = Mt. Avic, A = Antrona ophiolite, LM = Lanzo Massif; 4) Southalpine Domain: CA = Canavese Zone; 5) Oligocene Plutons: B = Biella, M = Miagliano, T = Traversella; 6) Lineaments: CL = Canavese Line, SF = Simplon Fault, AR = Aosta-Ranzola fault system.

A pre-Alpine polyphasic metamorphic evolution, from granulite- to amphibolite-facies conditions, is still preserved in marbles, metapelites, metagranitoids and metabasics (Castelli, 1991; Compagnoni *et al.*, 1977; Lardeaux *et al.*, 1982; Lardeaux & Spalla, 1991; Rebay & Spalla, 2001): the pre-Alpine T-climax has been constrained at T=730–830 °C P=0.7-0.9 GPa (Lardeaux & Spalla, 1991). Granulite- and amphibolite-facies imprints have been interpreted as the result of an extension-related uplift of a portion of the Variscan crust, occurred in Permian–Triassic times during the lithospheric thinning leading to the Tethys opening (e.g. Marotta & Spalla, 2007; Marotta *et al.*, 2009).

This pre-Alpine tectono-metamorphic evolution is preserved in the metamorphic complexes forming the SLZ: the Eclogitic Micaschist Complex (EMC), the Gneiss Minuti Complex (GMC), the II Dioritic–Kinzigitic Zone (IIDK) and the Rocca Canavese Thrust Sheets (RCT) (e.g.: Compagnoni *et al.*, 1977; Pognante, 1989a; Pognante, 1989b). The IIDK consists of kilometric lenses, lying between EMC and GMC, in which Alpine eclogitic assemblages are not described, though in the Vogna Valley the tectonic contact underlying the margin between IIDK and EMC is marked by eclogite-facies mylonites (Lardeaux, 1981; Lardeaux *et al.*, 1982). Eclogitic parageneses are widely described both in EMC and GMC with a strong difference in the volume affected by the greenschist re-equilibration: the GMC, which lies along the tectonic boundary with the Piedmont Zone, is widely re-equilibrated under greenschist facies conditions, while the EMC, constituting the internal part of the SLZ, records the greenschist-facies re-equilibration mainly along discrete shear zones and shows a dominant metamorphic imprint under eclogite-facies conditions (e.g. Spalla, 1983; Spalla *et al.*, 1991).

The EMC protoliths are high-grade paragneisses, granulites, amphibolites and minor marbles and quartzites, which are the country rocks of Permian granitoids and gabbros (Bussy *et al.*, 1998; Callegari *et al.*, 1976; Castelli, 1987; Cenki-Tok *et al.*, 2011; Compagnoni *et al.*, 1977; Oberhaensli *et al.*, 1985; Zucali, 2011) and
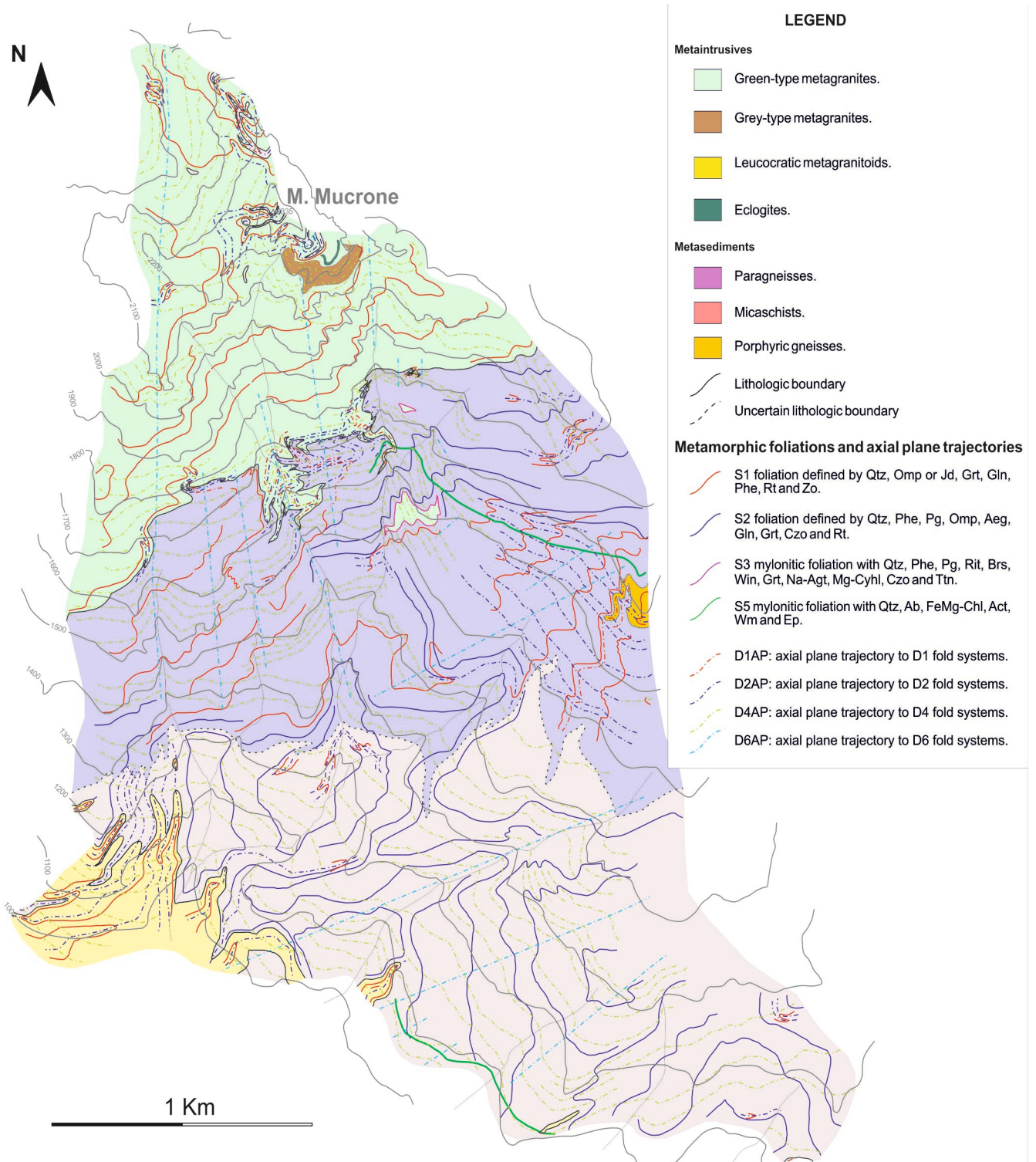
from which the Mt. Mucrone body is the most renown. The deformation history of EMC, in this area, comprises four generations of Alpine folds, two of which are associated with the high-pressure (HP) mineral assemblages, and two generations of shear zones synchronous with the blue- and greenschist-facies re-equilibrations, respectively (Hy, 1984; Zucali *et al.*, 2002b). According to earlier studies (Zucali, 2002) D1 and D2 deformations are generally associated with axial plane foliations marked by Ph, ±Pg, Na-Cpx, Grt, Rt and Zo (mineral abbreviations are used according to Whitney & Evans, 2010); the same mineral assemblage is stable during D3 folding. D4 is accompanied by a widespread re-equilibration under blueschist-facies conditions, confined along metre-wide mylonitic shear zones, which locally developed at the boundary between metagranitoids and country rocks. D5 mega-scale folds, D6 centimetre-thick mylonitic shear zones and gentle folding, overprinting blueschist mylonites and the eclogitic foliations, are synchronous with the formation of a typical greenschist-facies mineral association of Qz, Ab, Wm, Ep, Ttn and green-Amp.

Lithostratigraphy

In the Mt. Mucrone region the EMC consists of metagranitoids, mainly derived from Permian intrusives, and metasediments (mainly paragneisses and micaschists), descending from high-grade paragneisses that represent the country rocks of Permian intrusives, with minor metabasics.

The top of Mt. Mucrone, in the north-western sector of the studied area (Fig.2), mainly consists of Permian metagranitoids in primary contact with the hosts rocks (Maffeo, 1970; Oberhaensli *et al.*, 1985). Part of metagranitoids suffered only Alpine metamorphism, preserving the igneous structure (grey-type metagranitoids), whereas the others recorded also an intense Alpine deformation (green-type metagranitoids). The grey-type metagranites represent a small volume (< 20%) of the whole igneous Permian complex.

Figure 2. Structural map of the southern slope of Mt. Mucrone with foliation trajectories traced on standard lithological information.

LEGEND

Metaintrusives
- Green-type metagranites.
- Grey-type metagranites.
- Leucocratic metagranitoids.
- Eclogites.

Metasediments
- Paragneisses.
- Micaschists.
- Porphyric gneisses.

- Lithologic boundary
- Uncertain lithologic boundary

Metamorphic foliations and axial plane trajectories

- S1 foliation defined by Qtz, Omp or Jd, Grt, Gln, Phe, Rt and Zo.
- S2 foliation defined by Qtz, Phe, Pg, Omp, Aeg, Gln, Grt, Czo and Rt.
- S3 mylonitic foliation with Qtz, Phe, Pg, Rit, Brs, Win, Grt, Na-Agt, Mg-Cyhl, Czo and Ttn.
- S5 mylonitic foliation with Qtz, Ab, FeMg-Chl, Act, Wm and Ep.
- D1AP: axial plane trajectory to D1 fold systems.
- D2AP: axial plane trajectory to D2 fold systems.
- D4AP: axial plane trajectory to D4 fold systems.
- D6AP: axial plane trajectory to D6 fold systems.

M. Mucrone

1 Km

Relative chronology of superposed foliations (S1, S2, S3, etc.) is graphically represented by different colors of dashed lines. The inferred metamorphic conditions, under which successive foliations, folds and shear zones developed, can be inferred by the supporting mineral assemblages listed in the legend.

In the grey-type metagranitoids hypidiomorphic-granular primary textures are still recognizable, as well as compositional and grain size heterogeneities inherited from the igneous protoliths, consisting of: granites, minor quartzdiorites, pegmatites and aplites. In the poorly-deformed volumes the igneous contacts are generally preserved. Grey-type metagranites had a primary igneous composition consisting of: Qz (40%), Pl (35%), Kfs (15%) and Bt (10%). Only Bt, Kfs and rare Aln are partially preserved, while the Pl micro-site is totally replaced by Qz, Jd and Zo; Ph and Grt developed in coronas between Bt, Pl and Kfs. The grain size is medium and the texture is weakly porphyritic and the Bt content is ≤ 10%. Metaquartzdiorites generally occur in metre-thick boudins inside the grey-type metagranites; the main outcrop, a hundred meters wide, is embodied within the paragneisses (Fig. 2). This rock type is medium- to coarse-grained, with isotropic texture; the igneous structure is poorly preserved due to the widespread replacement of igneous phases by Alpine minerals: Omp (35%), Grt (25%), Qz (20%), white mica (10%) and Gln (10%). The inferred igneous modal composition with Pl (30%), Qz (20%), Kfs (10%) and mafic minerals (40%) is very close to that of a quartzdiorite or quartztonalite. Metaaplites and metapegmatites are fine-grained and coarse-grained rocks, respectively, with Jd, Grt and white mica and occur as centimetre to metre thick layers.

Green-type metagranitoids are fine- to medium-grained rocks with gneissic texture and a pervasive foliation underlined by white mica and clinopyroxene shape preferred orientations (SPO). These green coloured metagranitoids constituting about 80% of the Mt. Mucrone intrusives contain Jd or Omp, Grt, white mica and Gln. They do not show the same primary textural and compositional heterogeneities displayed by the grey-type metagranitoids, due to the strong textural and metamorphic reworking. These metagranitoids have been interpreted as a more deformed and mineralogically re-equilibrated (under eclogite facies conditions) equivalent of the "grey-type" ones (Castelli *et al.*, 1994). The most representative mineral association of the green-type metagranitoids is: Qz (30-50%), Na-Cpx (20-30%), white mica (15-20%), Grt (15-20%), Zo (5%) and Gln (5%). Leucocratic metagranitoids are exposed at the south-western margin of the mapped area and they do not show primary or deformed contact with the other metagranitoids. Generally they have a gneissic texture, without significant textural and

compositional variations, and are medium- to fine-grained with a penetrative foliation marked by white mica SPO and Qz-ribbons. The mineralogical composition is: Qz (40%), Ab (40%) and white mica (20%).

The metasediments consist of paragneisses and micaschists with interlayered minor metapegmatites, glaucophanites and zoisitites.

Paragneisses are medium-grained and show a mineralogical foliation marked by alternating Qz and Grt-layers, with Omp-Grt- and Gln-layers, parallelised to S1.

Metapegmatites (porphyric gneisses in the legend of Fig. 2) occur in metre-thick layers within paragneisses and contain coarse-grained Kfs porphyroclasts (20%), Qz (35%), Ab (25%) and white mica (20%). As already suggested in adjacent areas, they are interpreted as deformed and eclogitised leucosomes (Zucali, 2002; Zucali *et al.*, 2002b), deriving from pre-Alpine partial melting of the high grade gneisses (kinzigites). The dominant foliation in these gneisses is defined by white mica SPO and high strain of quartz-feldspar-bearing domains.

Micaschists are fine-grained rocks containing white mica, Qz, Grt, Gln and Jd or Omp. The dominant foliation (S1 in paragneiss and S2 in micaschists) is marked by alternating quartz- and mica-rich layers and has millimetre scale spacing. The boundary with the paragneisses is transitional, due to the large amount of mica in the highly-deformed paragneisses grading into the micaschists.

Metre to ten-metre thick glaucophanites occur in lenses or layers at the boundaries between micaschists and metagranitoids. They show a spaced foliation, marked by Gln SPO and cut by randomly oriented Omp porphyroblasts.

Zoisitites occur as ten-metre thick enclaves in the green-type metagranitoids and at the margin of the green-type metagranitoids; they contain ten centimetres-sized garnets, locally showing compositional zoning. The mineral mode of zoisitites is: Zo (35%), Qz (15%), white mica (10%), Omp (10%) and Grt porphyroblasts (30%). Ten-centimetre to metre-thick Qz-rich veins occur within metagranitoids and their country-rocks and contain minor amounts of white mica, Grt, Gln and Zo. Metabasics are medium- to fine-grained eclogites, locally showing a S2 discontinuous foliation, marked by Amp SPO. They are crosscut by millimetre- to centimetre-thick shear zone, rich in blue or green Amp. The mineral association is:

Omp (35%), Grt (25%), Gln (20%) Zo (10%), white mica (5%) and Qz (5%).

Mesostructure

Six groups of superposed ductile structures, named in the following D1 to D6, have been recognized during field mapping that was performed at 1:5.000 scale, with small areas mapped in greater detail (Delleani *et al.*, submitted). They are all syn-metamorphic and Alpine in age (Delleani *et al.*, 2010). Scattered pre-Alpine mineral and fabric relics (pre-D1) are preserved in domains in which the early Alpine deformation is poor or absent, mainly in metaintrusive rocks.
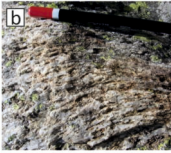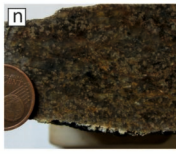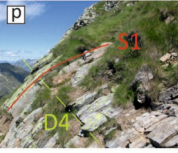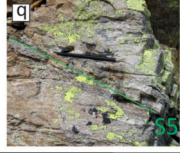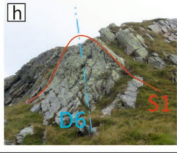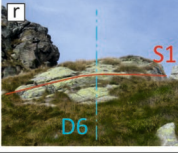
The interpretative map of Fig. 2 synthesises the structural framework reconstructed in accordance to various extent with the following criteria: i) fold style of similar rock multilayers: ii) kinematic compatibilities of fold systems; iii) interference patterns; iv) symmetry of minor folds; v) orientation of structures; vi) different assemblages marking foliations (e.g. Connors & Lister, 1995; Hobbs *et al.*, 1976; Johnson & Vernon, 1995; Passchier *et al.*, 1990; Passchier & Trouw, 2005; Spalla, 1993; Turner & Weiss, 1963; Williams, 1985). The geological boundaries have been traced on the interpretative map according to two classes of confidence: objective, indicated with solid lines, and interpretative with dashed lines, on the base of exposure and amount of structural data reported on the objective map (Delleani *et al.*, submitted). This map synthesizes the objective structural characters as foliation and fold axial surface trajectories, the sense of asymmetry of folds described by mineralogical or lithologic layerings, and interference patterns between superposed folds.

The degree of fabric evolution and peculiar structures developed during the successive metamorphic stages in metagranitoids and metasediments are shown in Figures 3 and 4, respectively.
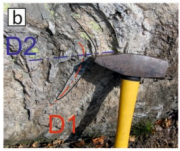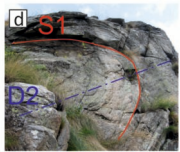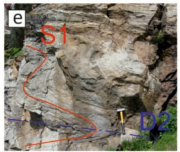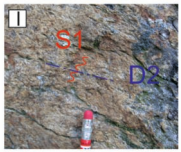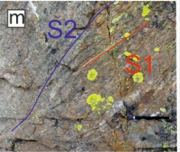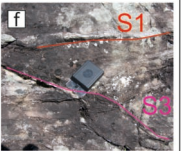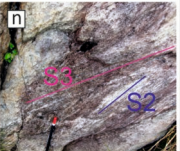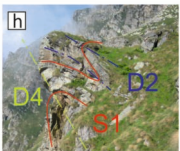
Figure 3. Representative structures characterising low, medium and high degree (LD, MD and HD, respectively) of fabric evolution during the successive deformation stages (D1-D6) in the two main types of metagranitoids.

	"grey type" metagranitoids			"green type" metagranitoids		
	LD	MD	HD	LD	MD	HD
D1	a		b	i		l
D2	c	d		m	n	
D3	e					o
D4	f			p		
D5			g			q
D6	h			r		

"Grey-type" metagranitoids: a) poorly-deformed, igneous texture in D1 LD; b) localized, progressive foliation developed close to a cm-thick syn-D1 mylonitic shear zone; c) poorly-deformed Qz igneous domains in D2 LD; d) D2 crenulation in hinge zone; e) weakly stretched igneous domains during D3; f) partially re-oriented igneous domains during D4 crenutal-ion; g) localized mm-thick shear zones in D5 HD domain; h) syn-D6 close fold. "Green-type" metagranitoids: i) 10-cm-spaced, discontinuous S1 foliation associated with D1 fold, emphasized by the contact with micaschists; l) mm-spaced S1 foliation and D1 fold, underlined by Qz-rich vein; m) syn-D2 parallel shape folding of S1; n) S1 + S2 composite fabric in D2 MD; o) mm-spaced S3 mylonitic foliation wrapping around 10-cm-thick eclogite boudin; p) gentle D4 folding with parallel shape; q) localized mm-thick shear zones in D5 HD; r) D6 gentle bending.

Figure 4. Representative structures characterising low, medium and high degree (LD, MD and HD, respectively) of fabric evolution during the successive deformation stages (D1-D6) in the two main types of country rocks.

Paragneisses: a) pre-Alpine compositional layering totally replaced by Amp-, Omp- and Grt-assemblages in poorly-deformed D1 domains; b) tight D1 folding of pre-Alpine alternating layers; c) mylonitic S1 foliation obliterating the pre-Alpine layering of paragneisses; d) parallel shape D2 folding; e) nearly isoclinal D2 folds with similar profile; f) cm-thick shear zone in D3 HD; g/h) open (g, LD) and tight (h, MD) D4 folds; i) cm-thick D5 shear zone in a Qz-rich layer of the paragneisses. Micaschists: l) rare preservation of continuous S1 foliation re-oriented by D2 crenulation; m) transposition of S1 foliation during the development of the new S2 axial plane fol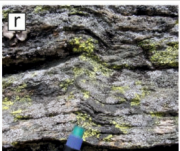iation; n) S2 foliation crosscut by S3 in D3 HD; o) D4 gentle folding; p) D4 crenulation in a micaschist re-equilibrated under greenschist facies conditions; q) numerous D5 mm-thick shear zones marked by whitish Ab and reddish Fe-oxides; r) D6 kink fold associated with the 10-m-wavelenght D6 gentle bending.

Pre-Alpine relics (pre-D1)

- Metaintrusive and metasedimentary rocks preserve some mineralogical pre-Alpine relics, such as Bt, Ksp, Aln, Ap and Zrn pre-Alpine relics within metagranitoids of Mt. Mucrone and pinkish Grt cores and Aln occur within micaschists and paragneisses. In low-deformed domains, metagranitoids (Fig. 3a) and paragneisses (Fig. 4a) preserve pre-Alpine structural relics such as inequigranular igneous texture. Primary igneous contacts between metre-thick aplitic and mesocratic dykes and metagranitoids are preserved.

Alpine deformations (D1-D6)

The first group of structures (D1) comprises isoclinal stretched similar folds and a pervasive axial plane foliation S1 (Figs. 3i, 3l, 4b and 4c), which is defined by SPO of Ph, Omp or Jd, Gln and Zo and by Grt-rich bands. S1 is a well-differentiated crenulation, showing a spaced to continuous character and is the most pervasive planar structure at the map scale in micaschists, paragneisses or metagranitoids. In metasediments, the degree of D1 fabric evolution ranges from stage 3 to stage 5 of the six stages decrenulation model of Bell and Rubenach (1983), whereas in metagranitoids it varies between stage 3 and 4 (Fig. 5) of the foliation development model of an originally isotropic rock, as described by Salvi *et al.* (2010).

D2 structures consist of isoclinal similar folds, metre to ten-metre in size, transposing the S1 foliation (Figs. 3c, 3d, 3m, 3n, 4d, 4e and 4l). An associated penetrative S2 foliation developed only in micaschists and is marked by SPO of Omp, Zo, Gln, Ph and Pg (Fig. 4m). In metasediments and metagranitoids the degree of D2 fabric evolution is similar to that of D1 stage, but the volume recording the more evolved stage of fabric development is sensibly smaller, as testified by the development of a penetrative foliation only in micaschists.

In poorly strained domains of metagranitoids, during deformation stages synchronous with the development of eclogite-facies assemblages, ten centimetre-thick shear zones developed (Fig. 3b), locally associated with Grt-bearing veins.

D3 structures principally consist of thick (up to 3 m) shear zones usually located at the main boundaries between different rocks (Fig. 3o). The associated S3 mylonitic foliation, occurring in these shear zones, is marked by Qz, Ph ± Pg, Amp ± Grt ± Chl, Czo and Ttn. Thicker shear zones locally occur along the boundaries between metagranitoids and country rocks, while in metagranitoids, paragneisses, eclogites and porphyric gneisses deformation and transformation are concentrated in cm-thick bands (Figs. 4f and 4n). During this stage, deformation is extremely localised and the degree of fabric evolution corresponds to stage 5-6, according to Bell & Rubenach (1983) and Salvi *et al.* (2010), in correspondence of

D3 shear zone but never exceed stage 2 in the rest of the area (Fig. 3e).

D4 structures comprise tight to open up to ten metre scale folds (Figs. 3p, 4g, 4h and 4o), associated with an intense crenulation in the hinge zone (Figs. 3f and 4p). These parallel folds represent the most recurrent fold system. Where the fabric evolution exceeds stage 2, the HP-minerals underlying the earlier fabric elements are replaced, to various extent (from 10 to 70%), by Ab, green Amp, Chl, Ep and a new generation of white mica. D4 folds range from metre to hundred meters in size with a weakly SW dipping axial plane. No new foliation develops during D4 folding: this deformation stage is associated with the growth of greenschist-facies minerals.

In the D5 centimetre-thick shear zones (Figs. 3g, 3q, 4i and 4q), S5 foliation is defined by Qz, Ab, Chl, green Amp, new white mica and Fe-Ep.

Large-scale D6 structures consist of gentle folds that appear as undulations of earlier structures at the hundred metre-scale (Figs. 3h, 3r and 4r). They are chronologically joined with brittle-ductile small fractures and joint systems filled by Chl, Ab and Kfs. D6 axial planes are marked by growth of very fine-grained dark Amp, white mica, Ab, Chl and Kfs (Adl).

The orientations of the fabric elements, plotted on the Schmidt diagrams of Table 1, suggest that the superposed fold systems (D2-D1, D4-D2 and D6-D4) generally have axial surfaces intersecting at a high angle, and fold axes intersecting at a low angle. These geometric relationships between the four fold groups are indicated by consistent interference patterns of type 3 (Ramsay, 1967) both at the outcrop and map scale (Figs. 2, 3 and 4).

1) S1 297 mesurements

2) S2 208 mesurements

3) D2 axial planes 105 mesurements

4) D2 axes 108 mesurements

5) S3 25 mesurements

6) D4 axes 104 mesurements

7) D4 axial planes 108 mesurements

8) S5 18 mesurements

9) D6 axes 10 mesurements

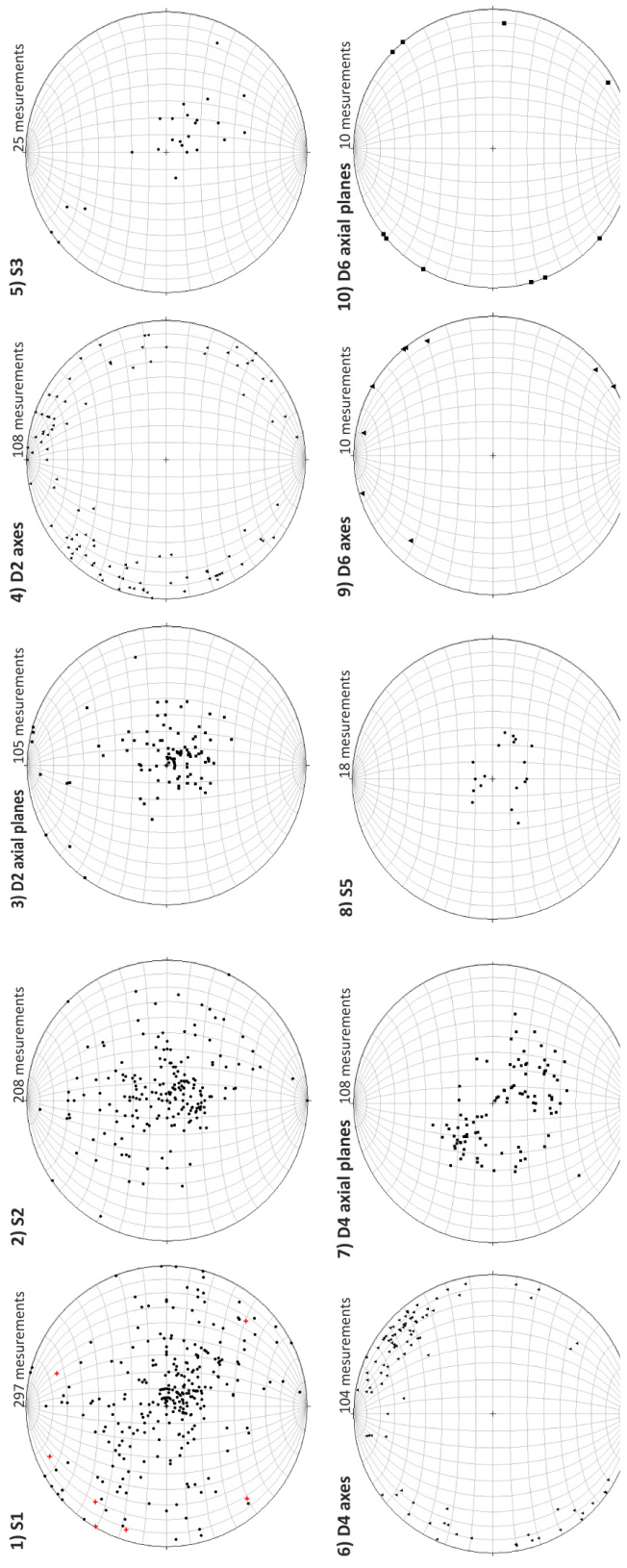**10) D6 axial planes** 10 mesurements

Table 1. Schmidt equal area diagrams of the structural elements (lower hemisphere): 1/2/3) The S1, S2 and D2 axial planes (synoptic Schmidt equal area diagrams) show a remarkable dispersion of data, due to superposition of deformation events (mostly by D2 and D4), with verticalization of surfaces in the hinge zones of the D2 and D4 folds; red crosses in the S1 diagram are poles to D1 fold axes. 4) D2 axes are sub-horizontal and do not display an orientation maximum; the dispersion of the D2 axes is influenced by non-cylindrical folding. 5) The distribution of S3 differs from that of S1 and S2 and admits reorientation by bending imposed during D4. 6) The D4 axes population forms a maximum at about 45-15°, and its weak dispersion reveals the effect of D6 fold axial surfaces striking 160°N that mainly imposes to the D4 axes a dip change from the NE to the SW. 7) The prevailing orientations of the axial planes of D4 are bimodal, with a maximum of up to 320°N, and dip about 30-40°; the second maximum is about 140°N, and dip about 20°. The D4 surfaces maxima are located on both sides of the successive D6 axial surfaces that strike 30-60°N or 160°N; the effect of the D6 axial planes striking 160°N is less clearly envisaged, due to the low angle between the average concentration of the D4 axial planes. 8) The S5 foliation planes are sub-horizontal. 9) The sub-horizontal D6 axes dip mainly to 40° and 160°N. 10) D6 folds display two preferred orientations of the subvertical axial surfaces striking 30-60°N and 160°N, respectively; these structures do not offer overprinting relationships and affect two separate rock volumes: the 30-60°N orientation prevails within the micaschists, leucocratic metagranitoids and finely foliated syn-D1 paragneisses (S and E map sectors), and the 160°N maximum occurs in the Mt. Mucrone metagranitoid and poorly deformed syn-D1 paragneisses.
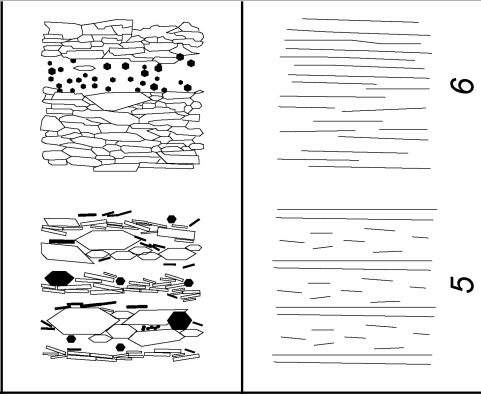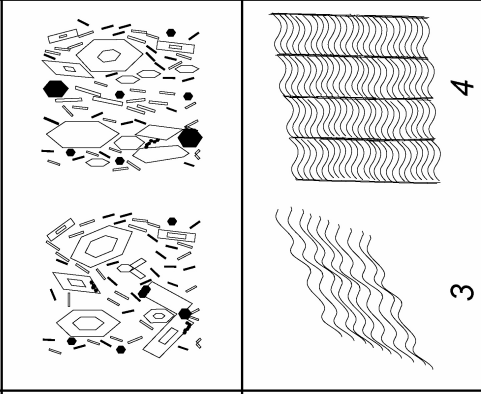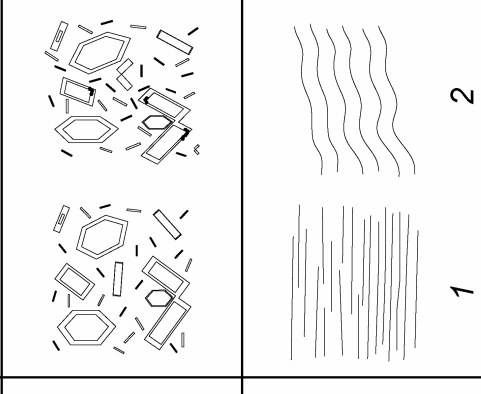
Microstructure

The interpretation of the Alpine structural and metamorphic evolution was based on the overprinting relationships indicated by the mesostructural study, linked with the petrographic evidences on the evolutionary sequence of parageneses supporting the microfabric changes. Deformation-metamorphism relationships have been inferred on the basis of the microstructural analysis of 93 thin sections, distributed over an area of ≈ 10 Km^2 (Fig. 2). During successive structural and mineralogical re-equilibration stages careful analysis of the effects of heterogeneous deformation made clear the contemporaneous development, in adjacent rock volumes, of equivalent mineral assemblages, manifest as different textures corresponding respectively with a low (LD = where the granular scale strain is extremely poor and is associated to metamorphic mineral growth localised at the rims of previous grains), medium (MD) and high degree (HD) of fabric evolution, respectively (Fig. 5).
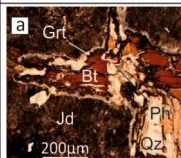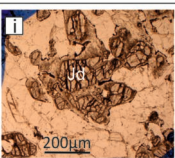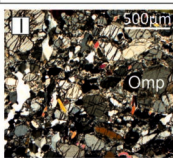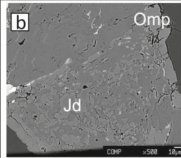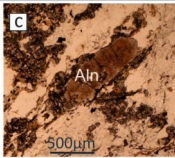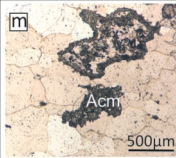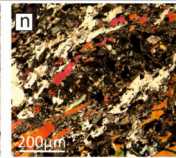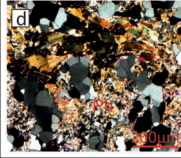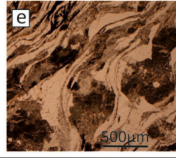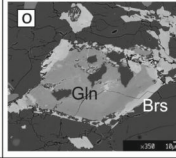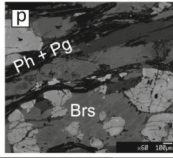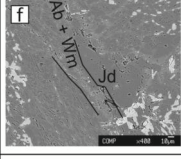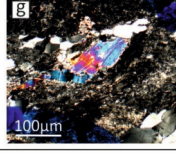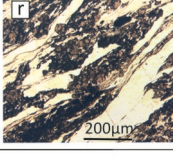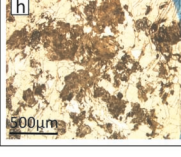
Examples of microfabrics characteristic of LD, MD and HD domains generated during successive deformation stages in metaintrusives and metasediments are shown in Figures 6 and 7, respectively.

Figure 5. Qualitative estimate of the degree of fabric evolution during foliation development, starting from originally foliated or initially isotropic rocks, as proposed by Salvi et al. (2010)
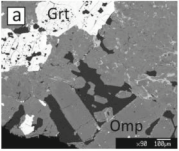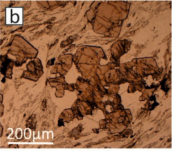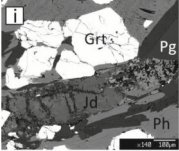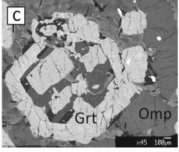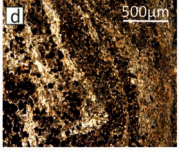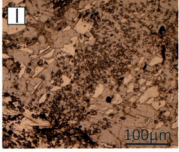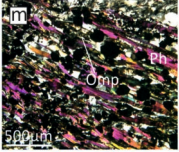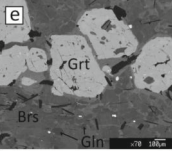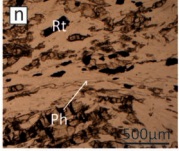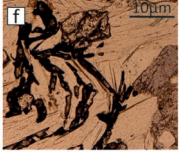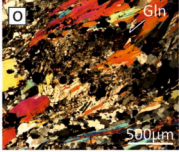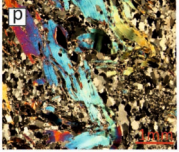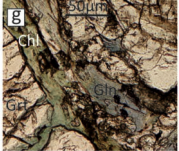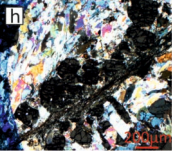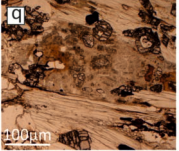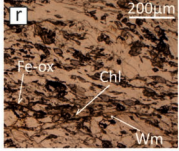
Italic numbers (1-6) of originally foliated rocks refer to the successive stages of crenulation cleavage evolution, up to complete decrenulation, as proposed by Bell and Rubenach (1983). The volume occupied by newly-oriented fabric elements, including the newly-differentiated mineral layering, is used to define the degree of fabric evolution, and to establish conventionally a low, medium or high degree of granular scale deformation (LD, MD and HD, respectively).

Figure 6. Representative microstructures of low, medium and high degree (LD, MD and HD, respectively) of fabric evolution during the successive deformation stages (D1-D5) in the two main types of metagranitoids.

| | "grey type" metagranitoids | | | "green type" metagranitoids | | |
	LD	MD	HD	LD	MD	HD
D1	a				i	l
D2	b	c		m	n	
D3	d		e	o		p
D4	f			q		
D5			g			r
D6	h					

"Grey type" metagranitoids: a) coronitic replacement of igneous Bt and Pl by eclogite-facies mineral as Cpx, Grt, Ph (plane polarized light); b) syn-D2 Omp rimming pre-D3 coronitic Jd – white mica aggregate (BSE image); c) S1+ S2 composite fabric wrapping Aln porphyroclast, associated with syn-D2 Grt and Ph partial re-crystallization (plane polarized light); d) fine-grained white mica growing after Jd aggregates in a poorly deformed domain close to D3 shear zone (crossed polars); e) syn-D1 localized mylonitic shear zone, reactivated during D3 with consequent flattening of Jd aggregates, partially replaced by fine-grained white mica (plane polarized light); f) replacement of syn-D4 Ab and Wm on the previous Jd, Qz and Zo aggregate, along old grain boundaries and microfractures (BSE image); g) very fine-grained re-crystallization of Ph along D5 shear plane (crossed polars); h) dark-Amp, Wm, Adl and Ab after Jd, Qz and Zo aggregates close to a D6 fold hinge (plane polarized light). "Green type" metagranitoids: i/l) incipient (i, plane polarized light) and well developed (l, crossed polars) S1 foliation marked by SPO of Na-Cpx grains; m) syn-D2 coronitic Acm rimming igneous Pl sites (plane polarized light); n) S1+S2 composite fabric associated with recrystallization of Ph, Na-Cpx and Qz (crossed polars); o) syn-D3 Brs rimming compositionally zoned Gln (BSE image); p) S3 foliation marked by Ph and Pg aggregates partially replacing older and coarser Ph and Brs (BSE image); q) Act and Wm filling of D4 fracture across syn-D2 Gln (plane polarized light); r) Na-Cpx stretched in a syn-D5 shear zone; Qz ribbon, new white mica and Chl overgrowing Cpx mark the mylonitic foliation (plane polarized light).

Figure 7. Representative microstructures characterising low, medium and high degree (LD, MD and HD, respectively) of fabric evolution during the successive deformation stages (D1-D6) in the two main types of country rocks.

Paragneisses: a) randomly oriented growth of Omp and Grt in an Amp-Omp-Grt-rich layer (BSE image); b) mm-spaced S1 foliation mainly marked by Ph SPO wrapping pre-Alpine Grt porphyroclasts (plane polarized light); c) atoll Grt in D2 LD domains, enclosing Ph, Pg and Gln (BSE image); d) D2 folding of S1 with bending of Grt- and white mica-rich layers; the latter is only partially re-crystallized (crossed polars); e) Brs partially replacing syn-D2 Gln in Amp-Omp-Grt-rich layer along mm-thick syn-D3 shear zone (BSE image); f) D4 microfolding of syn-D1 Ph with partial re-crystallization of Ph in new white mica and Ttn re-crystallisation (plane polarized light); g) Chl overgrew Grt and Gln in a MD domain close to D5 shear zone (plane polarized light); h) Ab and new white mica aggregates developed along syn-D5 shear plane (crossed polars). Micaschists: i) S1 foliation marked by Jd and Ph, whereas the timing of Pg growth is ambiguous and may post-date S1 (BSE image); l) coronitic growth of syn-D2 Gln enclosing a large amount of fine-grained Grt, Ph and Qz marking S1 (plane polarized light); m) S2 foliation marked by Ph and Omp SPO and by elongated Qz-domains with polygonal structure (crossed polars); n) S3 shear plane marked by Ph, with the formation of Ttn rims on Rt (plane polarized light); o) syn-D4 coronitic replacement of Gln by Ab, Wm, Ep and Act aggregates (crossed polars); p) D4 folding of syn-D1 Ph (crossed polars); q) very fine-grained aggregate of Ab and Wm developed on Na-Cpx during D5 (plane polarized light); r) Chl, Wm and Fe-oxides formation along D5 shear plane (plane polarized light).

Pre-Alpine relics (pre-D1)

Relics of the pre-Alpine mineral associations are widespread both in Mt. Mucrone metagranitoids and their country-rock. In metagranitoids, several igneous mineral relics have been preserved in LD and MD domains. They consist of: i) medium- to fine-grained brownish Bt (Fig. 6a), constituting up to 20% of the modal composition of grey-type metagranitoids; ii) medium-grained Aln (Fig. 6c) and Kfs (< 5% in volume) and rare, very fine-grained Ap and Zrn. Skeletal-shaped reddish Grt cores are pre-Alpine mineral relics in metagranitoid country rocks (Fig. 7b), well preserved in low D1 strain domains of paragneisses, and occasionally occurring in HD D1 domains. These Grt have numerous inclusions of fine-grained Qz, Ap and Rt. Medium-grained, pale-violet Aln relics occur also in paragneisses and zoisitites as in metagranitoids, whereas coarse-grained pinkish Mc occur in porphyric layers of the paragneisses.

As already pointed out, in poorly deformed domains pre-Alpine igneous relics are preserved in metagranitoids. However, most of these rock volumes are replaced by Alpine high pressure minerals. Poorly deformed metagranitoids consist of grey-type metagranitoids, metaaplites and metapegmatoids, in which the eclogite-facies minerals Jd, Ph, Grt and Zo replace as coronas more than 70% of the igneous assemblage (Fig. 6a). Pl is replaced by a fine-grained Jd-Qz-Zo aggregate, where colourless, randomly oriented and anhedral Jd, up to 3mm-sized encloses bubbly Qz and randomly-oriented acicular Zo; rare fine-grained Ph occurs within the symplectitic sites of plagioclase. Kfs is replaced by fine-grained and randomly oriented Ph crystals, and brownish Bt is only partially overgrown by fine- to medium-grained Ph. Coronas formed by trails of fine- to medium-grained Grt mark the margins between igneous Bt and Pl.

In paragneisses syn-D1 LD domains are characterised by randomly oriented growth of Omp and Grt in an Amp-Omp-Grt-rich layers (Fig. 7a).

Alpine microstructures (D1-D6)

Tectonitic to mylonitic syn-D1 foliations develop in both metaintrusive and metasedimentary rocks. In "green type" metagranitoids, metaaplites and metapegmatoids, cm- to 10-cm-spaced discontinuous S1 foliation is marked by syn-D1 Omp/Jd, Ph, Gln, Zo SPO and lenticular Qz-rich domains (Figs. 6i and 6l). The Omp/Jd forms euhedral coarse-grained crystals: in "green type"

metagranitoids and metapegmatoids Cpx is mostly pale green Omp, or more rarely Jd; in metaaplites only colourless Jd occurs. Medium- to coarse-grained Ph crystals enclose Qz and Rt with rational grain boundaries. The grain size of Ph and Cpx is coarser in metapegmatoids and "green type" metagranitoids. Grt trails are aligned parallel to the S1 foliation, and are formed by colourless or pale pink crystals with very fine-grained inclusions of Ap, Qz, Ph and Rt. Syn-D1 Grt are mainly fine-grained and with larger dimensions in highly strained domains (up to 5mm in diameter). Larger-sizes (up to 5cm) occur in Grt near the boundary between "green type" metagranitoids and zoisitites. In metaquarzdiorite, the 10- to 20 cm-spaced discontinuous S1 foliation is only locally preserved after D2 and D3 reworking: Omp, Ph, Zo SPO, elongated lenticular Qz domains and Grt trails mark S1. Omp has an internal foliation (Si) parallel and continuous with S1 and marked by SPO of fine-grained Ph and Zo and by small size Grt and Rt rows. In leucocratic metagranitoids and porphyric gneisses, scarce syn-D1 minerals are locally preserved within MD syn-D2 domains: coarse-grained Ph and rare fine-grained crystals of violet Gln and Zo with SPO parallel to S1. In porphyric gneisses, S1 is mainly underlined by coarse-grained Ph, Gln and Zo SPO, as in leucocratic metagranitoids, and wraps around Mc porphyroclasts showing recrystallized rims.

In syn-D1 HD domains the S1 foliation is generally continuous and has almost the same characteristics and mineralogical support in both micaschists and paragneisses, but in micaschists is only preserved within S2 microlithons. S1 is marked by SPO of medium-grained Ph, Gln Omp/Jd, Zo, by Grt strings and by mm- to cm-thick Qz lenses (Fig. 7i). Cpx generally is Omp, and Jd appeared only once. Ph is medium- to coarse-grained with inclusions of round-shaped Qz and euhedral Grt and Rt. Locally paragneisses are massive, with randomly oriented Omp, Gln, Zo and Ph occurring together with Grt and Qz in different modal amount within alternating layers. In glaucophanites S1 foliation is mainly preserved as Si in coarse-grained Omp and Grt and is marked by the alignment of Gln, Ph, Zo and accessory Rt. Omp and Grt porphyroblasts are interpreted as syn-tectonic with late D1, as suggested by gentle bending of their Si, and as pre-tectonic with respect to D2, as suggested by the relationships with S2, wrapping these porphyroclasts. In zoisitites the S1 foliation is mainly preserved as Si within Grt megablasts (up to 12 cm in diameter) and rare relicts

occur in the S2 microlithons within the matrix. S1 spaced foliation is marked by elongated lenticular Qz-domains and by SPO of fine-grained Czo, Ph, Gln and Omp.

During D2, normal foliations textures (S2) were imprinted exclusively in leucocratic metagranitoids, micaschists, eclogites, zoisitites and glaucophanites. Where D2 axial-planes intersect at a low angle, the S1 foliation acted as a microshear plane during D2, developing an S1-S2 composite fabric (of S-C type), accompanied by the growth of new fine-grained Ph crystals aligned in the foliations (Fig. 6n). In leucocratic metagranitoids relict S2 is marked by SPO of fine- to medium-grained Ph and Gln; Gln also defines L2. In micaschist the continuous S2 foliation is marked by SPO of Ph, Pg, Gln, Omp/Jd and Zo/Czo, by Grt trails and by Qz elongated lenses (Fig. 7m). Euhedral fine-grained Ph and Pg form new-grains from syn-D1 Ph or grew independently with long margins parallel to S2; light pink Grt rims syn-D1 Grt in microlithons, or define S2 with trails of euhedral fine-grained new grains. Fine-grained violet Gln elongated parallel to S2 may preserve pre-D2 pale cores, and up to 1cm long grains mark D2 axes (Fig. 7l). Omp/Jd and Zo/Czo can occur in rims of mm-thickness on the earlier Cpx and Zo grains.

S2 in eclogite is confined to 20cm-thick rims at the margins of boudinaged layers and is defined by SPO of fine- to medium-grained Omp and Ph, Pg and Grt rows. In D2 LD domains coarse-grained pale-green pre-D2 Omp grains with Grt, Ph and Rt inclusions have random orientations and colourless Grt occur also as medium grains with Rt and Ph inclusions. Oriented syn-D2 Omp developed from the re-crystallization of pre-D2 grains; thin coronas of rose Grt rims pre-D2 Grt. In zoisitites up to the 50% of the rock volume is replaced by new minerals during D2. Czo, Ph and Gln define S2, together with lens-shaped Qz-aggregates. In glaucophanites up to the 70% of the rock volume is replace by syn-D2 minerals and few Omp and Grt coarse-grained porphyroclasts occur. S2 foliation is supported by the alignment of Gln, Ph and Czo: fine-grained new grains of Gln replace pre-D2 crystals. Qz shows deformation bands, subgrains and polygonal new grains indicating syn-D2 dynamic recrystallization in LD domains of successive deformation stages in all rocks.

In D2 LD domains coronas of Omp, Grt, Gln, Ph and Czo rimming syn-D1 minerals never exceed 30% of the whole rock volume. Syn-D2 rims are mainly of < 1mm-thickness, regardless of the presence of an early oriented fabric. Within these rims inclusions are very rare, only locally very-fine grained Qz, Rt and Ap occurs. In metagranitoids and metapegmatoids fine-grained green-yellowish Acm coronas develop around Bt and Pl sites at the contact with Qz (Fig. 6m) and locally colourless Jd is partially replaced and rimmed by greenish Omp (Fig. 6b), randomly oriented and as very fine-grained needle-like crystals or very thin rims.

In cm- to m-thick D3 shear zones mylonitic texture developed in all rocks and are accompanied by the growth of new minerals replacing up to 50% of the previous mineral assemblages. In paragneisses poorly deformed during D1 the D3 deformation is localised in Qz- and Grt-bearing layers, thinned during this stage. In micaschists, zoisitites, glaucophanites and paragneisses, with a penetrative S1, D3 deformation is diffused, with no signs of concentration in shear zones, with a minor modal amount (<20%) of syn-D3 minerals. S3 is accompanied by grain size reduction and is marked by fine- to very fine-grained Qz elogated grains, SPO of Ph, Brs, Czo and by Ttn strings (Figs. 6d, 6e, 6o, 7e and 7p). In metaquartzdiorite fine-grained oriented Mg-Chl develops parallel to S3 or in pressure shadows of Omp porphyroclasts, very thin rims of Aug and Grt develop on pre-D3 Omp and Grt crystals and Ph + Pg aggregates replacing the earlier white mica grains are individuated at the electron microscope (Fig. 6p).

Generally, during D4, poor new minerals growth is observed and do not exceed the 20% of the whole rock volume in all lithologic types, with the exception of Ph-rich micaschists and leucocratic metagranitoids in which syn-tectonic mineral transformations could replace up to the 60% of the previous assemblages. Diffused fine-grained granoblastic Qz aggregates are associated with this deformation stage. Mineral transformations are mainly characterised by growth of fine- to medium-grained aggregates of Ab, new white mica, Ep and Act replacing older Amp (Figs. 6q and 7o), Na-Cpx (Fig. 6f) and Ph (Figs. 7f and 7p); within porphyric gneisses and micaschists Adl also occurs in these aggregates. Fe-Chl partially replaces Grt along boundaries and micro-fractures; green Bt partially overgrowing Ph and Grt may occur in paragneisses and micaschists.

During D5 mm- to cm-thick shear zones develop in all lithotypes and the new fabric (S5) is marked by fine- to

very fine-grained Qz, Ab, Wm, Act, green Bt, Ep, Ttn and Fe-oxides grain alignments (Figs. 6g, 6r, 7h and 7r). The same mineral association may occur in < 0.5 mm-thick veins with syntaxial filling. Aggregates of Ab, white mica, Ep and Act replace older Amp and Na-Cpx (Fig. 7q) and Fe-Chl partially replaces Grt along boundaries and micro-fractures (Fig. 7g), as already described for D4 microstructures. Transformations associated with D5 are localized along shear planes and never exceed 5% of the whole rock volume.

Mineral transformations are poor or absent within microstructures related to D6; they are a faint and variably spaced disjunctive axial plane foliation (fracture cleavage-type). Partial replacement of pre-D3 Jd aggregates by very fine-grained Ab, Wm, brown-Amp and Adl occurs locally in metagranitoids along the microfracture sets (Fig. 6h).

Fabric evolution vs reaction progress

The study of inter-relationships between the degree of planar fabric evolution and of metamorphic changes was respectively supported by structural maps of foliation trajectories (visualizing the history of superposed granular deformation imprints, Fig. 2), and by maps of degree of fabric evolution and metamorphic transformation domains (Fig. 8 and 9); the deformation history was derived from the structural study of the Mt. Mucrone metagranitoids (Delleani *et al.*, submitted), in which the chronology of superposed foliations (S1 to S5) and fold systems (D1 to D6) was inferred on the basis of overprinting criteria, aided by cross-controls of corresponding metamorphic assemblages.

Figure 8. Maps of the degree of fabric evolution (D1 and D2) and metamorphic transformation (M2) for D1 and D2 stages.
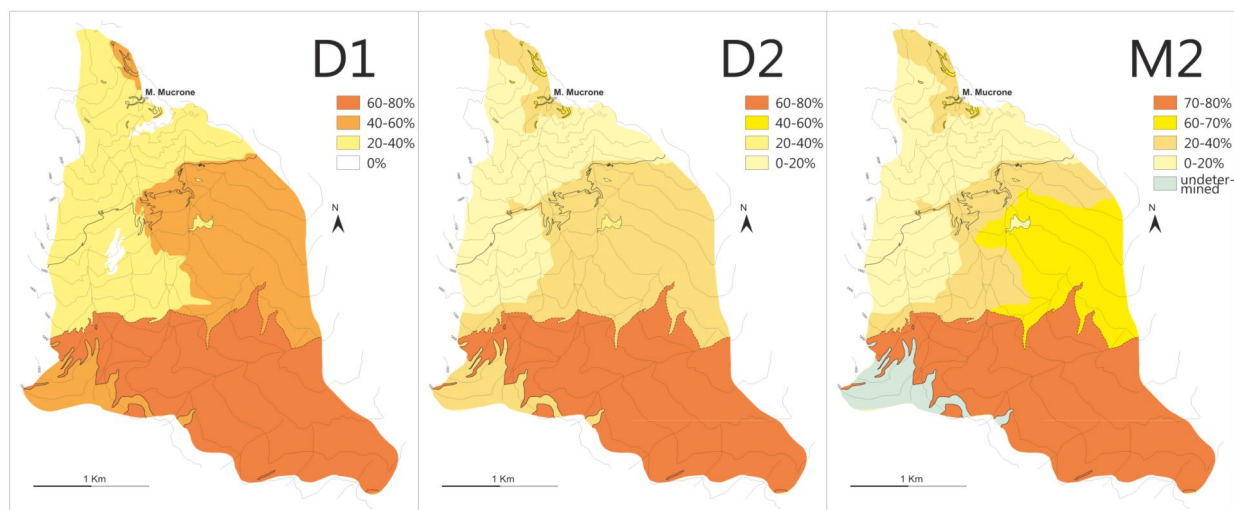
Syn-D1 mineral assemblages always constitute more than 70% of the rock volume. For this reason the map of the degree of metamorphic transformation is show only for D2 stage (M2). D1 HD domains are mainly localised in micaschists, leucocratic metagranitoids and in the eastern portion of the paragneisses. In metagranitoids syn-D1 HD domains mainly occur close to the boundaries with paragneisses (eastern portion of Mt. Mucrone southern slope) and micaschists (north of Mt. Mucrone).

Figure 9. Maps of the degree of fabric evolution (D3 and D4) and metamorphic transformation (M4) for D3 and D4 stages.
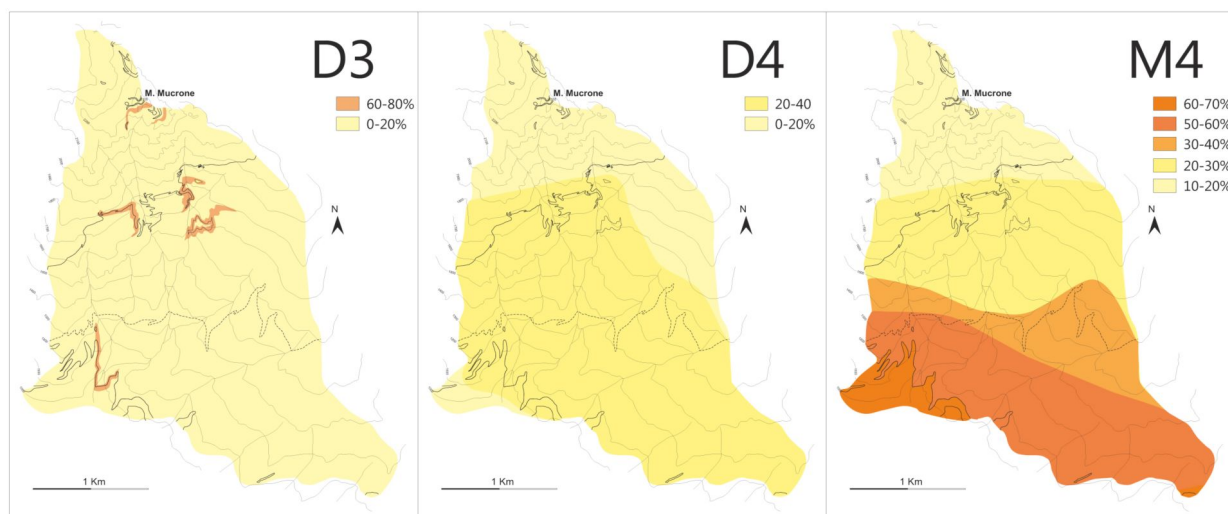
D3 mineral assemblages always constitute less than 10% of the rock volume in LD domains and no more than 60% in HD. For this reason the map of the degree of metamorphic transformation is show only for D4 stage (M4).

Individuation of homogeneous fabric domains was facilitated by integration of meso-structural information with microstructural analysis, from samples selected in accord with the deformation sequence. The degree of fabric evolution, indicating the volume percentage of new planar fabric, has been reconstructed together with the associated degree of syn-tectonic metamorphic transformations, indicating the modal amount of mineral assemblages expressed in percentage.

As already experienced by Salvi *et al.* (2010), the degree of grain-scale reorganization of the dominant fabric has been used as a guide to estimate the fabric evolution referring to the successive stages of crenulation cleavage development, as proposed by Bell & Rubenach (1983), from crenulation up to a complete transposition (see also Passchier & Trouw 2005). The scheme proposed by Salvi *et al.* (2010), elaborated starting from originally foliated or isotropic igneous fabric, has been adopted as a reference to discriminate between low-, medium- and high-deformation degrees (Fig. 5). This reference perfectly fits with the examined case of Mt. Mucrone, where, during Permian times, granitoids emplaced in polydeformed metapelites sharing since then the polyphase Alpine structural and metamorphic evolution.

Microstructural analysis showed that the discriminating intervals well fit with those proposed by Salvi *et al.* (2010) in which the low degree (LD) of deformation corresponds to the early development stage of the new fabric (volume of newly oriented fabric ranges from 0 to 20%) and includes an incipient crenulation or the appearance of a weak, non-persistent new foliation in country metapelites, and of no strain or a weak foliation in meta-intrusives, respectively; in other words this corresponds to the fabrics referred to as coronitic replacement.

The medium degree of deformation (MD) corresponds to a successive evolution up to the differentiation of a new foliation, which can reach the stage of a differentiated crenulation cleavage or a pervasive foliation (volume of newly differentiated fabric ranging from 20 to 60%), in originally foliated or isotropic rocks, respectively; this corresponds to the fabrics described above as tectonitic. The high degree of deformation (HD) coincides with the progressive obliteration of relicts of the earlier fabric in metapelites and metaintrusives and to development of a new continuous foliation of mylonitic type (volume of newly oriented fabric can rise up to 100%), thus corresponding to fabrics above described as mylonitic.

The estimate of volume percentage occupied by Alpine mineral assemblages syn-tectonic with successive deformation stages varies from 5 to 100%. Generally the higher is the degree of fabric evolution, the more pervasive is the mineral growth of the related syn-tectonic assemblages. The assemblages developed during D1, under eclogite-facies conditions, represent an exception: they

occupy a volume $\geq$ 90% in the mapped area, irrespectively of the degree of fabric evolution.

Disregarding D1 stage, LD is generally characterised by a volume of synkinematic metamorphic products ranging from 0 to 20% in metasediments (= originally foliated rocks). In metaintrusives (the only originally isotropic rocks), the relationships between degree of fabric evolution and metamorphic transformation is directly proportional, with a special case occurring during D4 in the leucocratic metagranitoids, outcropping at the southwestern margin of the map (Fig. 9), where the volume occupied by the Ph and Na-Cpx breakdown products rises up to 70%. MD domains show a volume of syn-tectonic metamorphic products varying from 20 to 70% both in originally foliated and in isotropic rocks. Finally, always with the anomaly of syn-D1 assemblages, in HD domains the mineral–chemical re-equilibration can reach up to 80% of the volume during D2 and never exceed 50% during D3: this latter represents the maximal degree of syn-D3 mineral replacement, which is generally < 10% in LD and MD syn-D3 domains.

Rock composition seems to exert an additional control on reaction progress, as can be inferred from Fig. 8 and 9, where the different modal amount of white mica and Na-Cpx influences the development of syn-D2 and syn-D4 metamorphic assemblages that are more pervasive in micaschists and leucocratic metagranitoids, respectively. In addition to original mineral rock composition and fabric evolution, the thermal regime can significantly influence the degree of metamorphic transformation where the fabric evolution remains below the HD stage: for the same degree of fabric evolution, the metamorphic reaction progress is more evolved during D2 (eclogite facies) than during D3 (blueschist facies).

The microstructural analysis results highlight that the two processes, degree of deformation and metamorphic transformation, do not necessarily develop at the same rate, but above the transition to the HD, the mechanical and mineral–chemical transformations of the rocks increase proportionally, in agreement with the observations of Salvi *et al.* (2010), Spalla *et al.* (2005) and Zucali *et al.* (2002b).

Mineral Chemistry

Mineral compositions have been determined within selected micro-structural sites in order to reveal the transformation pathways accompanying fabric evolution, and to support estimates of PT conditions during successive foliation-forming episodes and the related mineral equilibrations. Compositional variations in minerals have been determined using a Jeol, JXA-8200 electron microprobe (WDS, accelerating voltage of 15 kV, beam current of 15 nA) operating at the Earth Sciences Department "A. Desio" of Milano University. Natural silicates have been used as standards and the results were processed for matrix effects using a conventional ZAF procedure. Proportional formulae have been calculated on the basis of: 23 oxygens for Amp, 6 oxygens for Cpx, 12 oxygens for Grt and Ep, 11 oxygens for micas, 28 oxygens for Chl, 8 oxygens for Fsp and 10 for Ttn. Fe^{3+} was determined for Amp, Grt and Cpx; cations are in atoms per formula unit (a.p.f.u.). Mineral compositions synthesised below, are detailed in Table 2 and in diagrams of Figures 10-14, which show the compositional trends for mineral phases such as Amp, Cpx, Grt and white micas that are significant for thermobarometric estimates.

Amphiboles are scattered in composition over the edenite-hornblende, glaucophane, and actinolite fields. Most of them have edenite-hornblende compositions, and only a few data cluster around the glaucophane end-member, as shown in Figures 10a and 10c, where the compositional gap described by Ungaretti *et al.* (1983) between Ca- and Na-amphiboles, is evident only in metagranitoids and eclogites. Glaucophane is the most common composition for syn-D1 and syn-D2 amphiboles and only in a few cases amphiboles show an edenitic composition in "grey-type" metagranitoids and paragneisses. Syn-D3 compositions range from edenitic to pargasitic, whereas in syn-D5 the edenite content decreases up to actinolite composition. A decrease in Al^{VI} associated with an increase in Al^{IV} mark the transition from syn-D2 to syn-D3 amphiboles, whereas a strong decrease in Al^{tot} characterises the amphibole re-equilibration during D5 (Figs. 10b and 10d). Ti content generally ranges between 0.01 and 0.04 a.p.f.u. and Na(B) in NaCa-amphibole varies from 1.48 to 0.06 a.p.f.u. from syn-D3 to syn-D5, respectively.

Mineral	Amphibole					White Mica				Na-Clinopyroxene			Garnet					
Rock	Micas.	Micas.	Qzdior.	Parag.	Eclog.	"green" Gran.	"green" Gran.	Qzdior.	"grey" Gran.	"grey" Gran.	"green" Gran.	Eclog.	Parag.	Zoisit.	Mica.	Parag.	Mica.	Qzdior.
Defor. Stage	D1	D2	D3	D3	D4	D1	D2	D3	D5	D1 MD-HD	D1 LD	D2 MD-HD	pre-Alp.	progr. D1	D1 MD-HD	D1 LD	D2	D3
SiO_2	55.41	56.65	53.97	53.00	53.60	52.25	52.81	52.18	49.76	58.58	58.37	56.80	38.01	39.43	38.36	38.57	38.61	38.07
TiO_2	0.02	0.00	0.11	0.08	0.08	0.32	0.14	0.28	0.66	0.00	0.01	0.11	0.13	0.08	0.03	0.27	0.03	0.04
Al_2O_3	10.52	10.57	10.48	5.91	3.83	29.01	27.06	27.90	33.82	23.96	22.91	13.34	21.63	22.38	21.57	21.19	21.53	21.44
Cr_2O_3	0.00	0.00	0.02	0.01	0.05	0.00	0.00	0.00	0.07	0.00	0.00	0.01	0.00	0.00	0.02	0.05	0.01	0.03
FeO	13.90	12.91	13.08	9.68	11.94	2.14	3.05	3.42	1.34	1.62	3.41	4.15	29.42	19.89	30.70	20.05	24.97	25.74
MnO	0.05	0.07	0.10	0.07	0.10	0.01	0.01	0.00	0.05	0.01	0.01	0.02	2.86	0.56	0.60	1.48	0.30	1.01
MgO	7.96	8.36	10.47	14.98	15.29	2.92	3.12	2.58	0.98	0.20	0.04	6.29	3.91	7.10	4.31	1.42	4.83	2.66
CaO	1.37	0.65	5.51	9.81	12.45	0.00	0.00	0.00	0.03	0.83	1.19	10.73	4.79	10.87	4.53	17.65	9.69	10.68
Na_2O	6.35	6.95	4.74	2.25	0.56	0.90	0.40	0.66	0.17	14.62	14.25	8.57	-	-	-	-	-	-
K_2O	0.03	0.02	0.15	0.14	0.18	8.95	9.78	9.46	10.48	0.00	0.01	0.05	-	-	-	-	-	-
Total	95.61	96.19	98.64	95.93	98.07	96.49	96.37	96.47	97.37	99.82	100.20	100.07	100.75	100.32	100.12	100.68	99.96	99.68
Si	7.91	7.97	7.49	7.54	7.62	3.40	3.47	3.43	3.22	1.99	1.99	2.00	2.99	3.00	3.01	3.00	3.01	3.01
Ti	0.00	0.00	0.01	0.01	0.01	0.02	0.01	0.01	0.03	0.00	0.00	0.00	0.01	0.00	0.00	0.02	0.00	0.00
Al	1.77	1.75	1.71	0.99	0.64	2.23	2.09	2.16	2.58	0.96	0.92	0.55	2.01	2.00	2.00	1.94	1.98	2.00
Cr	0.00	0.00	0.00	0.00	0.01	0.00	0.00	0.00	0.00	0.00	0.00	0.00	0.00	0.00	0.00	0.00	0.00	0.00
Fe^{3+}	0.17	0.20	0.54	0.50	0.22	0.12	0.17	0.19	0.07	0.02	0.04	0.03	0.00	0.00	0.00	0.03	0.01	0.00
Fe^{2+}	1.49	1.32	0.98	0.65	1.21	-	-	-	-	0.02	0.06	0.09	1.94	1.27	2.04	1.27	1.61	1.71
Mn	0.01	0.01	0.01	0.01	0.01	0.00	0.00	0.00	0.00	0.00	0.00	0.00	0.19	0.04	0.04	0.10	0.02	0.07
Mg	1.69	1.75	2.17	3.18	3.24	0.28	0.31	0.25	0.09	0.01	0.00	0.33	0.46	0.80	0.50	0.16	0.56	0.31
Ca	0.21	0.10	0.82	1.50	1.90	0.00	0.00	0.00	0.00	0.03	0.04	0.40	0.40	0.88	0.38	1.47	0.81	0.90
Na	1.76	1.90	1.28	0.62	0.15	0.11	0.05	0.08	0.02	0.96	0.94	0.58	-	-	-	-	-	-
K	0.01	0.00	0.03	0.03	0.03	0.74	0.82	0.79	0.87	0.00	0.00	0.00	-	-	-	-	-	-

Recalculated components:

Amphibole

	D1	D2	D3	D3	D4
$Al^{(VI)}$	0.09	0.03	0.52	0.46	0.38
$Al^{(IV)}$	1.68	1.72	1.20	0.53	0.26
$Na_{(M4)}$	1.76	1.90	1.18	0.50	0.10

White Mica

	D1	D2	D3	D5
$Al^{(VI)}$	1.63	1.56	1.59	1.8025
$Al^{(IV)}$	0.60	0.53	0.57	0.778

Na-Clinopyroxene

	D1 MD-HD	D1 LD	D2 MD-HD
Q	3.21	5.30	41.44
Jd	94.56	90.97	55.63
Ae	2.23	3.73	2.93

Garnet

	pre-Alp.	progr. D1	D1 MD-HD	D1 LD	D2	D3
Alm	64.79	42.40	68.81	41.62	53.48	57.06
Py	15.33	26.85	17.00	5.55	18.78	10.47
Grs	13.50	29.54	12.78	47.71	26.36	30.12
Sps	6.37	1.20	1.34	3.28	0.66	2.26
Adr	-	-	-	1.68	0.69	-

Table 2. Representative compositions of Amp, Cpx, Grt and Wm in micaschists (= Micas.), paragneisses (= Parag.), eclogites (= Eclog.), zoisitites (= Zoisit.), metaquartzdiorite (= Qzdior.), grey-type metagranitoids (= "grey" Gran.) and green-type metagranitoids (= "green" Gran.).

Figure 10. Compositional range of amphiboles from metaintrusives (a, b) and metasediments (c, d).
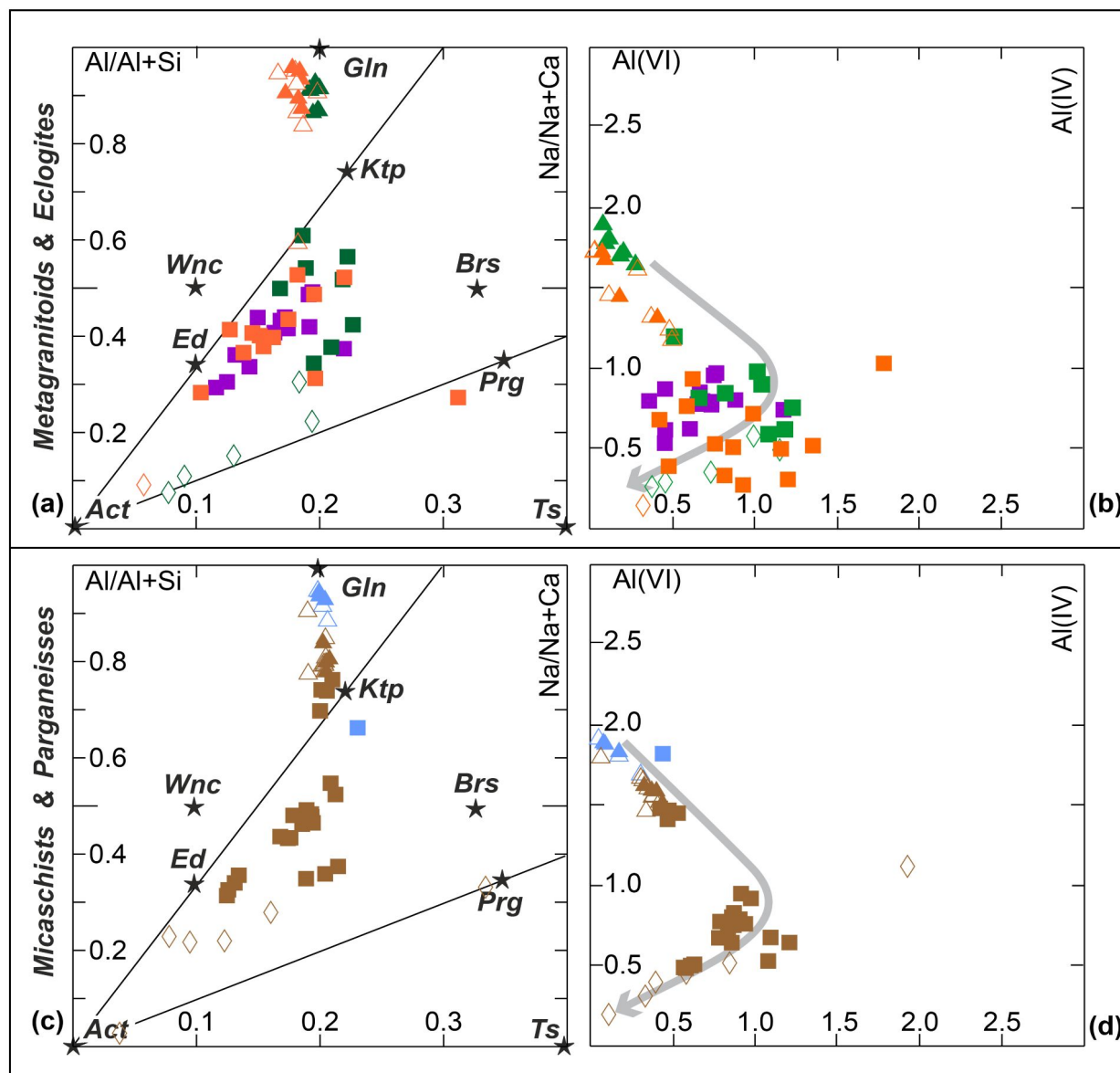
Stars locate end-member composition (Act = actinolite; Brs = barroisite; Ed = edenite; Gln = glaucophane; Ktp = kato-phorite; Prg = pargasite; Ts = tschermakite; Win = winchite). Straight lines define the amphibole trends for high and inter-mediate pressure, from Vermont (Laird & Albee, 1981). Amphibole composition trends during Alpine evolution is shown by the grey arrows on the Al(VI) vs Al(IV) diagrams (b, d). Different colors identify rock types and simbols deformation stages: grey-type metagranitoids in red; green-type metagranitoids in orange; eclogites in green; metaquartzdiorites in violet; micaschists in light-blue; paragneisses in brown; D1 = full triangle; D2 = open triangle; D3 = full box; D4 = open box; D5 = open diamond. Full triangle identifies pre-D3 grains in eclogites.

Clinopyroxenes vary in composition from Jd to Di, in a range from Jd98, to Jd15 (Fig. 11). The highest acmitic values occur in Cpx from some "grey-type" metagrani-toids. Jd-content in both grey and green metagranitoid types, is also controlled by the bulk chemistry as shown by the two clusters of pre-D3 and syn-D1 and D2 grains in Figure 11. In green-type metagranitoids and in

eclogites a weak increase in Jd and a decrease in Acm contents characterise the transition from syn-D1 to syn-D2 Cpx. Similarly, a Jd increment characterises the tran-sition from syn-D1 to syn-D2 Cpx compositions in para-gneisses and micaschists. A higher Di content distin-guishes post-D3 Cpx, both in eclogites and paragneisses.

X_{Mg} varies from 0.01 to 0.62 with higher values in syn-D3 grains.

Garnets, as inferred microstructurally, grew during both Alpine and pre-Alpine metamorphic evolutions, and pre-Alpine relics have been recognized in paragneisses (open circles in Fig. 12 and zoning profile in Fig. 13). The transition from pre-Alpine to Alpine syn D1-D2 garnets is characterised by an Alm, Sps and Adr decrease and a Grs and Prp increase. The transition from syn-D1 to syn-D2 Grt in paragneisses is marked by a Sps decrease associated with a Grs increase, while Grt occurring in micaschists (Fig. 12) shows an homogeneous composition with Alm 65-70, Prp 10-20 and Grs 15-25; also syn-D1 Grt megablasts in zoisitites (Fig. 13) show a quite uniform compositional profile. The strong heterogeneous composition of pre-D3 garnets in "grey-type" metagranitoids is due to their microstructural position. As already described, these Grt develop in coronas at the boundary between Pl and Bt sites and the highest Grs values occur in Grt growing on the Pl site from those replacing Bt, that are characterised by higher Alm+Prp contents (Figs. 12 and 13), as already described by Koons *et al.* (1987). Grt filling the veins at high angle with mylonitic foliation in D1 shear zones are characterised by very low amounts of Prp and Sps (<5%). In green-type metagranitoids and metaquartzdiorite, the Alm+Prp content decreases and Grs increases characterise the transition from syn-D1 to syn-D2 compositions. In eclogites, Alm ranges from 60 and 65%, Prp from 10 and 20%, Grs from 20 to 30 % and Sps is <5%.

Figure 11. Pyroxene compositions according to Morimoto (1988) for Cpx in metaintrusives and metasediments.

Different colors identify rock types and simbols deformation stages: grey-type metagranitoids in red; green-type metagranitoids in orange; eclogites in green; metaquartzdiorites in violet; micaschists in light-blue; paragneisses in brown; D1 = full triangle; D2 = open triangle; D3 = full box; D4 = open box; D5 = open diamond. In grey-type metagranitois full triangle identifies pre-D3 grains. See discussion in the text.

http://virtualexplorer.com.au/

Figure 12. Garnet compositional variations in metasediments and metaintrusive rocks.
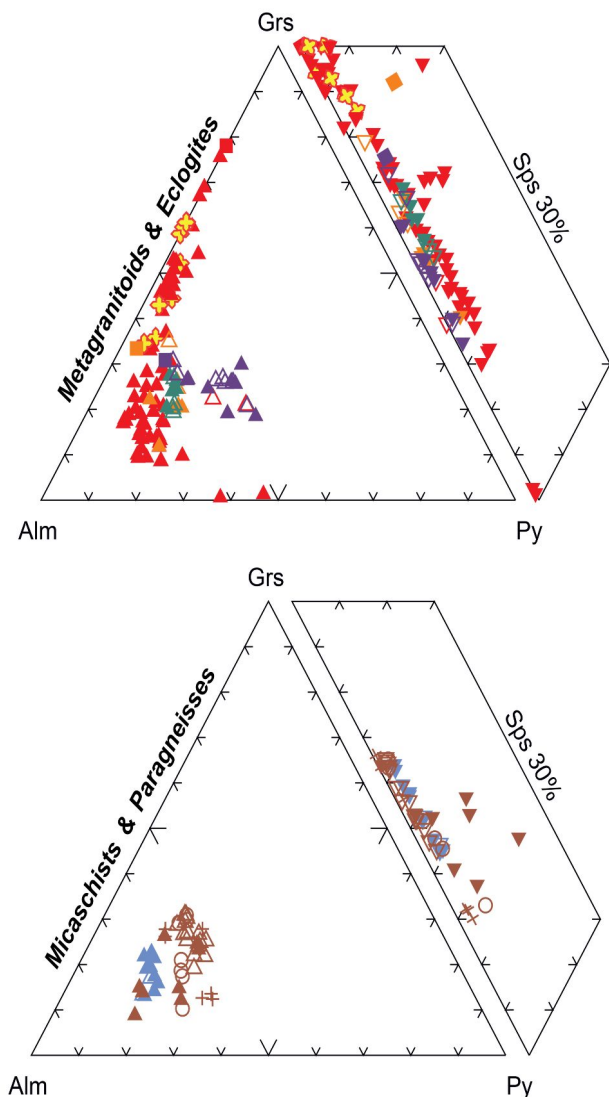
Different colors identify rock types and symbols deformation stages, respectively: grey-type metagranitoids in red; green-type metagranitoids in orange; eclogites in green; metaquartzdiorites in violet; micaschists in light-blue; paragneisses in brown; D1 = full triangle; D2 = open triangle; syn-D1 veins = yellow cross; D3 = full box; D4 = open box; D5 = open diamond. In grey-type metagranitois full triangle identifies pre-D3 grains. See discussion in the text.

Figure 13. Examples of compositional zoning in Grt from pargneisses, zoisitites and grey-type metagranitoids.
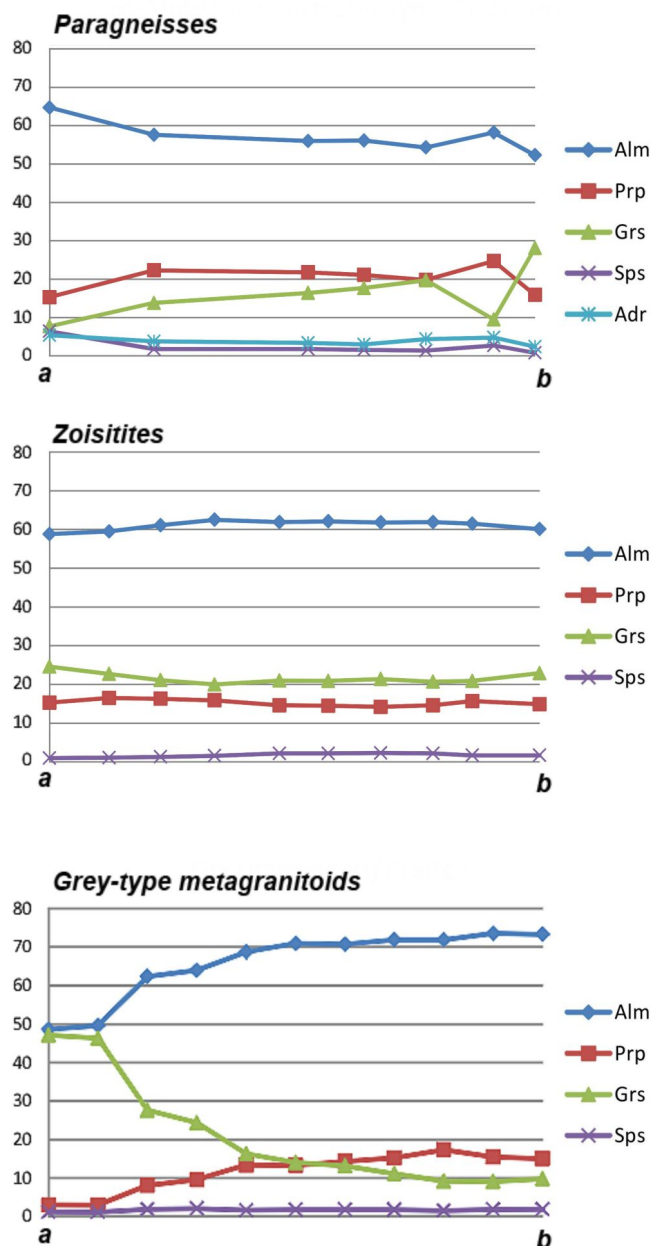
Paragneisses: zoning from pre-Alpine core (a: pre-D1) to Alpine rim (b: syn-D1-D2). Zoisitites: Rim-to-rim (a to b) compositional profile across a syn-D1 megablast. Grey-type metagranitoids: variations in composition across a Grt corona developed between the Pl (a) and Bt (b) site.

White micas consist of paragonite and phengite (Fig. 14) with Ca never exceeding 0.03 a.p.f.u.; K content in paragonite is up to 0.09 a.p.f.u., whereas Pg is ≤ 0.13 a.p.f.u. in phengite. Eclogites contain phengitic micas that show the highest Si^{4+} content (3.35–3.55 a.p.f.u.),

with the highest values in syn-D2 grains. In metagranitoids, Si^{4+} varies from 3.2 to 3.5 a.p.f.u. from syn-D5 to syn-D1/D2 grains. In metasediments, the compositional variations in Ph are lower than those of metaintrusives ($3.35 < Si^{4+} < 3.45$ a.p.f.u.). Mg values are 0.25-0.4 a.p.f.u. in Ph from metasediments and more scattered (0.2-0.8 a.p.f.u.) in those from metaintrusives, where a higher variation in the Fe^{3+} content is suggested by the deviation

from the Ph-Lc trend in the diagram (Fig. 14) of Massonne & Schreyer (1987). Ti content does not exceed the value of 0.24 a.p.f.u.: in grey-type metagranitoids $0.10 < Ti < 0.24$ a.p.f.u. where Ph replaces igneous Bt and $Ti \leq 0.10$ a.p.f.u. in all the other micro-sites.

Figure 14. Phengite compositions in metasediments and intrusive rocks displayed in the ternary diagram of Massonne & Schreyer (1987) and in the Si/Mg (in a.p.f.u.) plot.
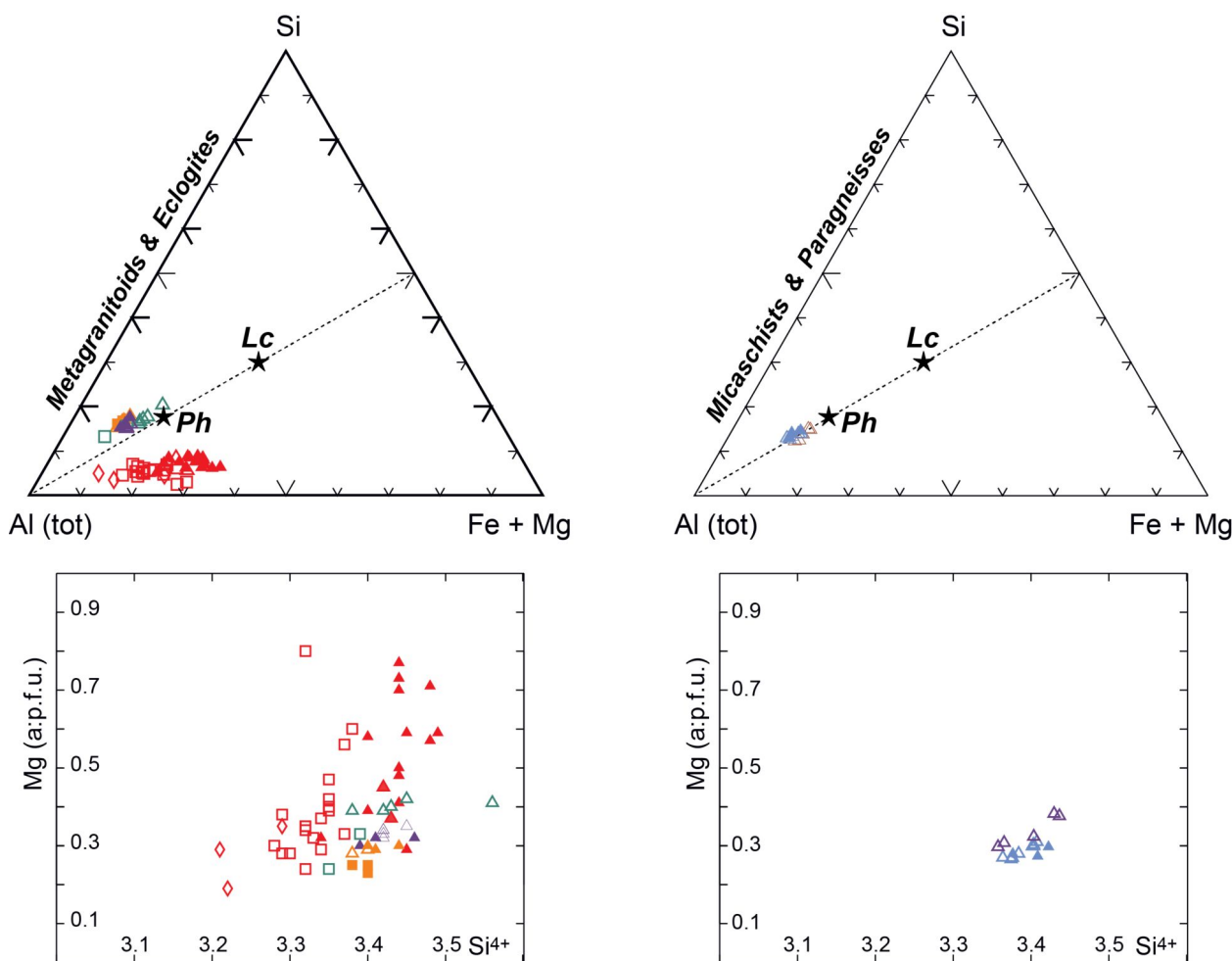
Stars locate end-member composition (Ph = phengite; Lc = leucophyllite). Different colors identify the rock types and symbols the deformation stages: grey-type metagranitoids in red; green-type metagranitoids in orange; eclogites in green; metaquartzdiorites in violet; micaschists in light-blue; paragneisses in brown; D1 = full triangle; D2 = open triangle; D3 = full box; D4 = open box; D5 = open diamond. In grey-type metagranitois full triangle identifies pre-D3 grains. In metagranitoids a higher content in Fe3+ is suggested by the deviation from the Ph-Lc tie-line.

Chlorite has X_{Mg} values between 0.73 and 0.48 and Si ranges from 2.78 to 2.98 a.p.f.u.; Mg-richer Chl occurs in metaquartzdiorites. *Epidotes* shows Fe_2O_3 up to 15.93

wt.% and MnO is lower than 0.21 wt.%; generally syn-D3 Ep are Czo and pre-D3 Zo, whereas greenschist-facies epidote are Fe-Ep. *Alpine plagioclase* has An < 0.05 and Or < 0.01 and titanite has Al_2O_3 ranging from 2.03 to 2.11 wt %.

P-T estimates and metamorphic evolution

Micro-structural analysis indicates that the Mt. Mucrone rocks preserve evidence of superposed metamorphic and structural re-equilibrations, even at thin section scale, and allows definition of assemblage sequences in metapelites and metagranitoids, syn-tectonic with successive deformation stages. To infer PT conditions active during each metamorphic re-equilibration, favourable sites where microstructures suggest the attainment of grain-scale equilibrium have been identified. For this purpose, samples dominated by a single structural and metamorphic imprint at thin section scale have been selected, to obtain internally coherent PT estimates, using independent thermo-barometers. Even so, metamorphic conditions inferred using critical minerals such as Grt, for which the compositional zoning suggests a heterogeneous re-equilibration with the matrix assemblage, have been calculated selecting mineral pairs with textural relationships indicating equilibrium. We also considered that mica, Cpx and Amp grains associated with different fabric elements in the same rock, may have different chemical compositions, reflecting different intra- and intercrystalline deformation mechanisms, as it has been demonstrated under various metamorphic conditions (e.g. Buatier & Lardeaux, 1987; Cimmino & Messiga, 1979; di Paola & Spalla, 2000; Gazzola *et al.*, 2000; Lardeaux *et al.*, 1983; Spalla, 1993; Spalla & Zucali, 2004). This makes these minerals proper to estimate the physical conditions during the development of successive fabrics. PT conditions of each re-equilibration stage have been inferred using: a) the comparison of natural assemblages with experimental univariant equilibria; b) calculation of average PT using the THERMOCALC package (Holland & Powell, 1998; Powell & Holland, 1994) based on specific mineral compositions; c) the application of well-calibrated, independent thermometers and barometers: calibrations have been applied taking into account the best fit between the compositional range of mineral pairs in different samples.

Mineral assemblages marking successive groups of structures (Tab. 3) indicate that D1 and D2 occurred under eclogite facies conditions, D3 under blueschist-facies conditions and D4 to D6 under greenschist facies conditions. In *metagranitoids* the integrated use of AX and average PT routines of THERMOCALC gives P = 1.9 ± 0.3 GPa and T = 479° ± 50° C for syn-D1 assemblage Gln-Omp-Grt-Ph-Zo (with Qz in excess), P = 2.6 ± 0.3 GPa and T = 522° ± 45° C for syn-D2 assemblage Gln-Omp-Grt-Ph-Pg-Zo (with Qz in excess), P = 1.4 ± 0.4 GPa and T = 515° ± 45° C for syn-D3 assemblage Brs-Grt-Czo-MgChl-Ph-Di-rich Cpx (with Qz in excess). Temperatures have also been estimated using the Fe-Mg exchange between garnet and white mica (Wu *et al.*, 2002) stable during D2 at 586° ± 49° C. Si^{4+} content in pre-D3 Ph ranges from 3.4 and 3.5 a.p.f.u., covering the same composition interval obtained in Ph synthetized under HP condition in metatonalitic systems at P ≥ 2.0 GPa (Schmidt, 1993). In *eclogites*, average PT calculations on the assemblage Omp-Gln-Grt-Ph-Zo-Qz, stable during D1, gives P = 1.9 ± 0.5 and T = 504° ± 150° C. Temperatures have been evaluated using the Fe-Mg exchange between garnet and clinopyroxene marking D1 fabric at T = 488° ± 25° C for P = 1.4 – 2.3 GPa (Krogh Ravna, 2000). Variation in garnet compositions from syn-D1 to syn-D2 grains, if compared with experimental results at high pressure on metabasalts (Poli, 1993), indicates P ranging from 2.0 to 2.2 GPa, in agreement with D1-D2 P-interval estimated with average PT also in metagranitoids. In *micaschists* and *paragneisses* the garnet - white mica thermometer applied to syn-D2 mineral pairs gives T = 554° ± 49° C and T =597° ± 44° C, respectively. The coexistence of actinolitic amphibole (Al^{tot} = 0.2 – 0.9 a.p.f.u.) with albite (An ≤ 0.05) during D5 in paragneisses allows the evaluation of P ≤ 0.4 GPa and T ≤ 400°C (Plyusnina, 1982). The inferred PT values for the different syn-tectonic assemblages perfectly justify the variations of mineral chemical compositions, such as: i) CaNa-amphiboles, in which the evolution from syn-D1/D2 to syn-D3 grains is marked by a decrease in Al^{tot} and Na; ii) the increase of Jd-content in Cpx grains from D1 to D2; iii) the decrease of Si^{4+} content in Ph, from syn-D1 to syn-D5; iv) Grt zoning.

These results on the chemistry of single minerals, constituents of the successive fabrics, are compatible with the sequence of syn-tectonic assemblages and are synthesized in the Pressure-Temperature-deformation-time (PTdt) path diagram of Fig. 15 showing that the structural evolution from D1 to D2 occurred during a P-prograde path, characterised by a slight T-increase. D2 deformation assisted the P-T climax conditions and was followed by decompression at quite constant T, characterising D3 conditions. Syn-D4 greenschist-facies mineral assemblages and the syn-D5 PT estimates indicate that the last

deformation stages developed during a significant T-decrease, associated with decompression.

Lithologic type	pre-Alpine	D1	D2	D3	D4	D5	D6
Grey-type metagranite	Bt+Aln+Zrn+Ap+Qz	Jd+Qz+Ph+Grt+ Zo+Rt	Omp+Acm+Qz+Ph+ Pg+Grt+Gln+Czo+Rt	Qz+Ph+Pg+Brs+ Czo+Ttn	Qz+Ab+Wm+Act+ Ttn+Bt+Ep	Qz+Ab+Wm+Act+ Ttn+Bt+Ep+Fe-Ox	Ab+brown-Amp+ Wm+Adl
Metaquartz-diorite	Aln+Qz	Omp+Gln+Qz+Ph+ Grt+Zo+Rt	Omp+Acm+Qz+Ph+ Pg+Grt+Gln+Czo+Rt	Qz+Ph+Pg+Brs+Aug+ Mg-Chl+Czo+Ttn	Qz+Ab+Wm+Act+ Ttn+Bt+Ep	Qz+Ab+Wm+Act+ Ttn+Bt+Ep+Fe-Ox	-
Metaaplite	Bt+Aln+Zrn+Ap+Qz	Jd+Qz+Ph+Grt+ Zo+Rt	Omp+Acm+Qz+Ph+ Pg+Grt+Gln+Czo+Rt	Qz+Ph+Pg+Brs+ Czo+Ttn	Qz+Ab+Wm+Act+ Ttn+Bt+Ep	Qz+Ab+Wm+Act+ Ttn+Bt+Ep+Fe-Ox	Ab+brown-Amp+ Wm+Adl
Metapegmatoid	Bt+Aln+Zrn+Ap+Qz	Jd±Omp+Qz+Ph+Grt+ Zo+Rt	Omp+Acm+Qz+Ph+ Pg+Grt+Gln+Czo+Rt	Qz+Ph+Pg+Brs+ Czo+Ttn	Qz+Ab+Wm+Act+ Ttn+Bt+Ep	Qz+Ab+Wm+Act+ Ttn+Bt+Ep+Fe-Ox	Ab+brown-Amp+ Wm+Adl
Green-type metagranitoid	Zrn+Aln	Omp±Jd+Qz+Ph+Grt+ Gln+Zo+Rt	Omp+Acm+Qz+Ph+ Pg+Grt+Gln+Czo+Rt	Qz+Ph+Pg+Brs+ Czo+Ttn	Qz+Ab+Wm+Act+ Ttn+Bt+Ep	Qz+Ab+Wm+Act+ Ttn+Bt+Ep+Fe-Ox	-
Leucocratic metagranitoid	-	Ph+Gln+Zo+Rt	Ph+Gln	Qz+Ph+Pg+Brs+ Czo+Ttn	Qz+Ab+Wm+Act+ Ttn+Bt+Ep	Qz+Ab+Wm+Act+ Ttn+Bt+Ep+Fe-Ox	-
Eclogite	-	Omp+Grt+Gln+Ph+ Zo+Rt	Omp+Grt+Ph+Pg+ Rt+Zo	Qz+Ph+Pg+Brs+ Czo+Ttn+Aug	Qz+Ab+Wm+Act+ Ttn+Bt+Ep+Di-Cpx	Qz+Ab+Wm+Act+ Ttn+Bt+Ep+Fe-Ox	-
Paragneiss	Grt+Qz+Rt+Aln+Ap	Omp+Ph+Grt+Qz+ Gln+Zo+Rt	Omp+Ph+Pg+Grt+ Qz+Gln+Czo+Rt	Qz+Ph+Pg+Brs+ Czo+Ttn	Qz+Ab+Wm+Act+ Ttn+Bt+Ep+Di-Cpx	Qz+Ab+Wm+Act+ Ttn+Bt+Ep+Fe-Ox	-
Micaschist	Grt+Qz+Rt+Ap	Omp±Jd+Qz+Ph+Grt+ Gln+Zo+Rt	Qz+Ph+Pg+Omp±Jd+ Grt+Gln+Zo±Czo	Qz+Ph+Pg+Brs+ Czo+Ttn	Qz+Ab+Wm+Act+ Ttn+Bt+Ep+Adl	Qz+Ab+Wm+Act+ Ttn+Bt+Ep+Fe-Ox	-
Porphyric gneiss	Mc	Qz+Ph+Mc+Gln+ Zo+Rt	Qz+Ph+Gln+Czo+Rt	Qz+Ph+Pg+Brs+ Czo+Ttn	Qz+Ab+Wm+Act+ Ttn+Bt+Ep+Adl	Qz+Ab+Wm+Act+ Ttn+Bt+Ep+Fe-Ox	-
Glaucophanite	-	Gln+Ph+Zo+Rt	Omp+Grt+Ph+ Czo+Qz+Rt	Qz+Ph+Pg+Brs+ Czo+Ttn	Qz+Ab+Wm+Act+ Ttn+Bt+Ep	Qz+Ab+Wm+Act+ Ttn+Bt+Ep+Fe-Ox	-
Zoisitite	Aln	Grt+Zo+Ph+Omp+ Gln+Rt	Qz+Czo+Ph+Gln+Rt	Qz+Ph+Pg+Brs+ Czo+Ttn	Qz+Ab+Wm+Act+ Ttn+Bt+Ep	Qz+Ab+Wm+Act+ Ttn+Bt+Ep+Fe-Ox	-
Qz-bearing vein	-	Ph+Omp+Qz+Grt+ Gln+Zo+Rt	Qz+Grt+Omp+Ph+ Gln+Czo+Rt	Qz+Ph+Pg+Brs+ Czo+Ttn	Qz+Ab+Wm+Act+ Ttn+Bt+Ep	Qz+Ab+Wm+Act+ Ttn+Bt+Ep+Fe-Ox	-

Table 3. Mineral assemblages marking successive fabrics in the different lithotypes of Mt. Mucrone lithostratigraphy.

Figure 15. PT paths inferred for the Mt. Mucrone rocks
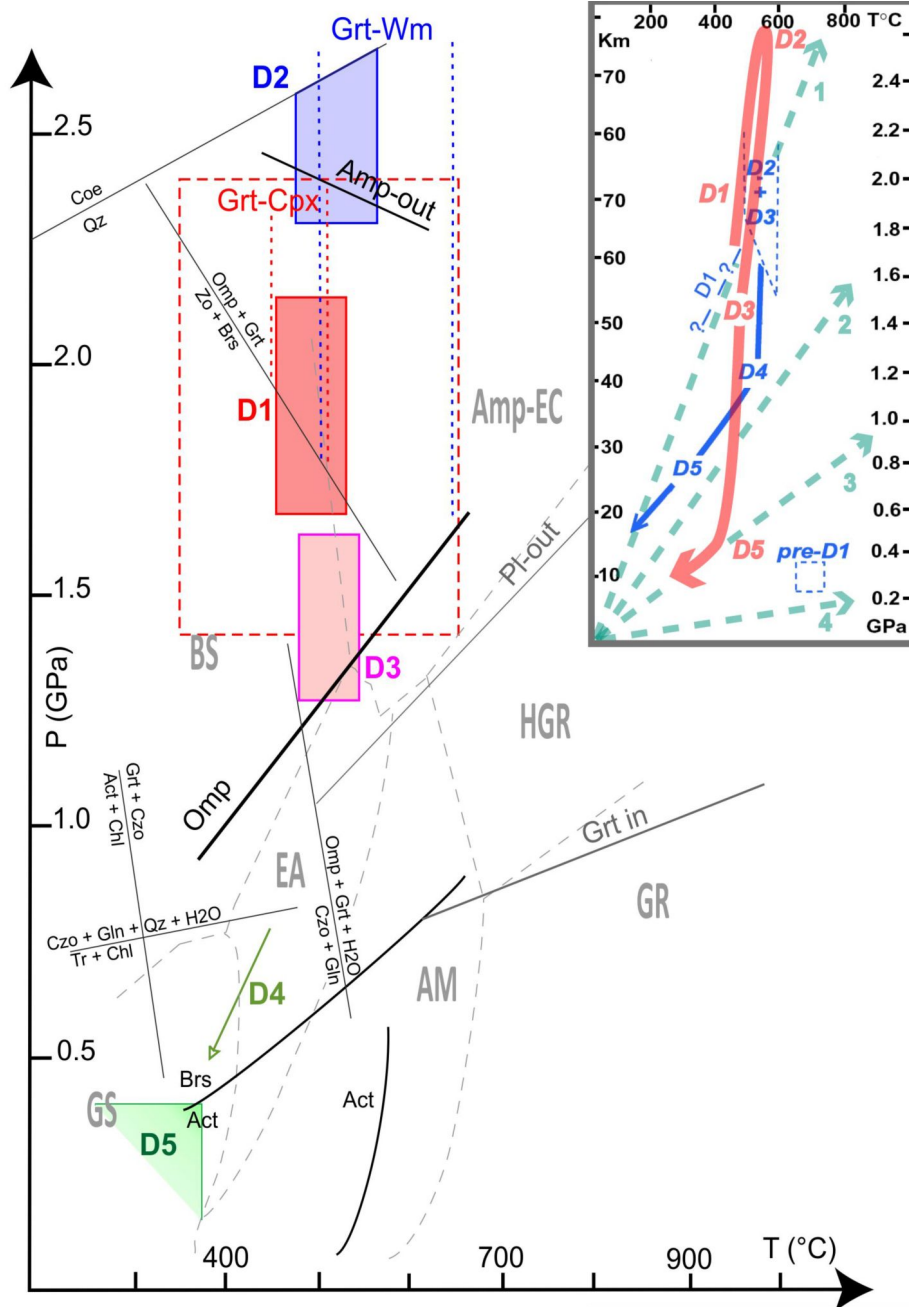
Boxes represents the average PT estimates performed with AX and average PT routines of THERMOCALC in metagranitoids (colored boxes) and eclogites (dashed box). Red dashed lines represents T-intervals estimated with the Grt-Amp thermometer in eclogites. Blue dashed lines represents T-intervals estimated with the Grt-white mica thermometer in micaschists and paragneisses. Green open triangle locates the evaluation of syn-D5 conditions in paragneisses. Metamorphic facies (Ernst & Liou, 2008): GS = greenschist; EA = epidote-amphibolite; BS = blueschist; AM = amphibolite; Amp-EC = amphibole-bearing eclogite; HGR = high pressure granulite; GR = granulite. Brs/Act transition (Ernst, 1979); Act/Hbl transition (Moody et al., 1983); Omp-in and Amp-out (Poli & Schmidt, 1995); Pl-out and Grt-in (Liu et al., 1996). In the inset, the inferred PTdt path (orange) is compared with that of Zucali et al. (2002), shown in blue. Ligth-green lines are geotherms: 1) "cold" subduction zones, 2) "warm" subduction zones, 3) normal gradient of old plate interior, 4) near spreading ridge or volcanic arc (Cloos, 1993).

Conclusive remarks

Multiscale structural analyses performed in a portion of the subducted-exhumed Alpine continental crust evidenced that the accomplishment of syn-tectonic polyphase metamorphic transformations was controlled not only by bulk and mineral compositions, but was also variably influenced by fabric evolution, as shown by the maps of degree of fabric evolution and metamorphic transformation. This result agrees with the conclusions obtained in other portions of the Alpine continental crust, variably reworked in the Mesozoic-Tertiary subduction (Roda & Zucali, 2008; Salvi *et al.*, 2010; Spalla *et al.*, 2000; Spalla *et al.*, 2005; Zucali *et al.*, 2002b). The heterogeneity of Alpine deformation assisted the preservation of volumes dominated by relics of igneous textures, even where magmatic minerals were widely replaced by Alpine eclogitic assemblages. The detailed structural and petrographic mapping allowed reconstruction of the tectonic and metamorphic evolutionary steps of the Permian granitoids of the Mt. Mucrone southern slope, back to the nearly undeformed igneous textural relics.

The correlation between degree of fabric evolution and reaction progress in different lithotypes has shown that the differences of mineral assemblages and textures of the protoliths influenced the reaction accomplishment when the degree of fabric evolution remains lower than HD, as discussed in the section *"Fabric evolution vs reaction progress"*. Maps of volumetric estimates of mineral transformation, compared with those showing the diffusion of granular scale deformation throughout the rock indicate, as already proposed by Salvi *et al.* (2010), that the HD stage represents a threshold after which deformation and metamorphism effects proportionally increase up to the total replacement of pre-existing minerals where new fabrics evolved up to the stage of a continuous foliation. These observations call attention on the role of strain energy in catalysing metamorphic reactions (Hobbs *et al.*, 2010).

In addition the evaluation of metamorphic reaction progress for the same degree of fabric evolution, during successive deformation stages, suggests that also the metamorphic environment exerts an influence as indicated by the more widespread development of eclogite-facies assemblages (syn-D2) with respect to the blueschist-facies (syn-D3) or greenschist-facies ones (syn-D4).

Finally, strain gradients may induce variations in lithostratigraphy as in the case of: i) transformation of the grey-type into green-type metagranitoids, as a consequence of deformation and mineral replacement intensity during syn-eclogitic stages, or ii) the transformation of paragneisses into micaschists localized along syn-D1 HD domains. Caution is therefore suggested in the use of lithostratigraphy as an independent key to contour tectonic units in polydeformed and polymetamorphic terrains, without the support of the multiscale structural and petrographic analysis.

Structural and metamorphic evolution point to the development of D1 and D2 stages under PT conditions of the Qz-eclogite facies not far from the boundary with the Coe stability field, of D3 stage under blueschist-facies conditions, and of D4-D6 stages under greenschist-facies conditions (Fig. 15).

Peak conditions attained during D2 (T = 480°-580° C and P = 2.3 – 2.7 GPa) were accomplished after a P and T prograde path during which the Mt. Mucrone metagranitoids and their country rocks recorded D1 deformation at T = 430° - 530°C and P = 1.9 ± 0.3 GPa. The retrograde path is marked by a transition to T = 470° - 560°C and P = 1.4 ± 0.4 GPa during D3, and successively re-equilibrated under greenschist-facies conditions up to P ≤ 0.4 GPa and T ≤ 400° C (syn-D5 re-equilibration). This structural and metamorphic history predates the emplacement of Oligocene dykes, indicating that these rocks were exhumed to greenschist-facies conditions before Tertiary magmatic activity, in agreement with the exhumation time suggested for adjacent areas of SLZ, also on the basis of the structural relationships with Biella and Traversella intrusive stocks (Zanoni, 2010; Zanoni *et al.*, 2008; Zanoni *et al.*, 2010; Zucali, 2002; Zucali *et al.*, 2002a). The age of deformation history recorded under eclogite-facies conditions can be estimated between 90 and 65 Ma according to U/Pb determinations on Aln and Zrn (Cenki-Tok *et al.*, 2011; Rubatto *et al.*, 1999). The inferred PTdt evolution is in good agreement with that deduced by Zucali *et al.* (2002) for the Mt. Mucrone-Mt. Mars area (Fig. 15), but minimal P climax conditions attain higher values of 2.3 GPa and P is constrained at maximum values of 2.7 GPa by the Coe stability field.

To conclude, D1 and D2 stages are characterised by a P/T ratio lower than that of cold subduction zones (Cloos, 1993), whereas D3 falls in this thermal state of about 6°C/Km, indicating that this part of the structural and metamorphic history has been recorded in a scenario

of active subduction of a cold and old oceanic plate. Post-D3 exhumation took place under a thermal state comprised between those corresponding to warm subduction zones and plate interior (Cloos, 1993), therefore compatible with continental collision.

Acknowledgements

References

Babist, J., Handy, M.R., Konrad-Scmolke, M. and Hammerschmidt, K. (2006). Precollisional, multistage exhumation of subducted continetal crust: the Sesia Zone, Western Alps. Tectonics, 25:10.1029/2005TC001927

Bell, T.H. and Rubenach, M.J. (1983). Sequential porphyroblast growth and crenulation cleavage development during progressive deformation. Tectonophysics, 92: 171-194. 10.1016/0040-1951(83)90089-6

Bigi, G. Castellarin, A., Coli, M., Dal Piaz, G.V., Sartori, R., Scandone, P. and Vai, G.B. (1990). Structural Model of Italy, sheets 1-2. In: Progetto Finalizzato Geodinamica del C.N.R. S.E.L.C.A., Florence.

Buatier, M. and Lardeaux, J.M. (1987). Intracrystalline deformation of omphacite and garnet under high-pressure and low-temperature conditions - example from the Sesia-Lanzo Zone (Western Alps). Comptes Rendus Academie des Sciences (Series II), 305(9): 797-800.

Bussy, F., Venturini, C., Hunziker, J. and Martinotti, G. (1998). U-Pb ages of magmatic rocks of the Western Austroalpine Dent Blanche-Sesia Unit. Schweizerische Mineralogische und Petrographische Mitteilungen, 78: 163-168.

Callegari, E., Compagnoni, R., Dal Piaz, G.V., Frisatto, V., Gosso, G. and Lombardo, B. (1976). Nuovi affioramenti di metagranitoidi nella zona Sesia-Lanzo. Rendiconti della Società Italiana di Mineralogia e Petrologia, 32: 97-111.

Castelli, D. (1987). Il metamorfismo alpino delle rocce carbonatiche della Zona Sesia-Lanzo (Alpi occidentali). PhD Thesis, Università di Torino, 141 pp.

Castelli, D. (1991). Eclogitic metamorphism in carbonate rocks: the example of impure marbles from the Sesia - Lanzo Zone, Italian Western Alps. Journal of Metamorphic Geology, 9: 61-77. 10.1111/j.1525-1314.1991.tb00504.x

Castelli, D., Compagnoni, R. and Nieto, J.M. (1994). High pressure metamorphism in the continental crust: eclogites and eclogitized metagranitoids and paraschists of the Monte Mucroen area, Sesia Zone. In: High pressure metamorphism in the Western Alps. Guide-book to the B1 field excursion of the 16th Gen. IMA Meeting, Pisa, 4-9 settembre 1994, 107-116.

Castelli, D. and Rubatto, D. (2002). Stability of Al and F-rich titanite in metacarbonate: petrologic and isotopic constraints from a polymetamorphic eclogitic marble of the internal Sesia Zone (Western Alps). Contributions to Mineralogy and Petrology, 142: 627-639. 10.1007/s00410-001-0317-6

Cenki-Tok, B. Oliot, E., Rubatto, D., Berger, A., Engi, M., Janots, E., Thomsen, T.B., Manzotti, P., Regis, D., Spandler, C., Robyr, M. and Goncalves, P. (2011). Preservation of Permian allanite within an Alpine eclogite facies shear zone at Mt Mucrone, Italy: Mechanical and chemical behavior of allanite during mylonitization. Lithos, 125: 40-50. 10.1016/j.lithos.2011.01.005

Cimmino, F. and Messiga, B. (1979). I calcescisti del Gruppo di Voltri (Liguria occidentale): le variazioni composizionali delle miche bianche in rapporto all'evoluzione tettonico-metamorfica alpina. Ofioliti, 4(3): 269-294.

Cloos, M. (1993). Lithospheric buoyancy and collisional orogenesis: subduction of oceanic plateaus, continental margins, island arcs, spreading ridges and seamounts. Geological Society of America Bulletin, 105: 715-737. 10.1130/0016-7606(1993)105<0715:LBACOS>2.3.CO;2

Compagnoni, R. (1977). The Sesia-Lanzo zone: high-pressure low-temperature metamorphism in the Austroalpine continental margin. Rendiconti della Società Italiana di Mineralogia e Petrologia, 33: 335-374.

Compagnoni, R., Dal Piaz, G.V., Hunziker, J.C., Gosso, G., Lombardo, B. and Williams, P., 1977. The Sesia-Lanzo Zone: a slice of continental crust, with alpine HP-LT assemblages in the Western Italian Alps. Rendiconti della Società Italiana di Mineralogia e Petrologia, 33: 281-334.

Connors, K.A. and Lister, G.S. (1995). Polyphase deformation in the western Mount Isa Inlier, Australia; episodic or continuous deformation? Journal of Structural Geology, 17(3): 305-328. 10.1016/0191-8141(94)00057-7

Dal Piaz, G.V. (1999). The Austroalpine-Piedmont nappe stack and the puzzle of Alpine Tethys. Memorie di Scienze Geologiche, Padova, 51: 155-176.

Dal Piaz, G.V., Hunziker, J.C. and Martinotti, G. (1972). La Zona Sesia - Lanzo e l'evoluzione tettonico-metamorfica delle Alpi Nordoccidentali interne. Memorie della Società Geologica Italiana, 11: 433-460.

Delleani, F., Castelli, D., Spalla, M.I. and Gosso, G. (2010). The record of subduction-related deformation in the Mt. Mucrone metagranitoids (Sesia-Lanzo Zone, Western Alps). Rendiconti online Società Geologica Italiana, 10: 46-49.

Delleani, F., Spalla, M.I., Castelli, D. and Gosso, G. (submitted). A new petrostructural map of Monte Mucrone metagranitoids (Sesia-Lanzo Zone, Western Alps). Journal of Maps.

Di Paola, S. and Spalla, M.I. (2000). Contrasting tectonic records in pre-Alpine metabasites of the Southern Alps (Lake Como, Italy). Journal of Geodynamics, 30: 167-189. 10.1016/S0264-3707(99)00032-0

Ernst, W.G. (1979). Coexisting sodic and calcic amphiboles from high pressure metamorphic belts and the stability of barroisitic amphibole. Mineralogical Magazine, 43: 269-278. 10.1180/minmag.1979.043.326.09

Ernst, W.G. and Liou, J.G. (2008). High- and ultrahigh-pressure metamorphism: Past results and future prospects. American Mineralogist, 93: 1771-1786. 10.2138/am.2008.2940

Gazzola, D., Gosso, G., Pulcrano, E. and Spalla, M.I. (2000). Eo-Alpine HP metamorphismin the Permian intrusives from the steep belt of the central Alps (Languard-Campo nappe and Tonale Series). Geodinamica Acta, 13: 149-167. 10.1016/S0985-3111(00)00115-7

Gosso, G. (1977). Metamorphic evolution and fold history in the eclogite micaschists of the upper Gressoney valley (Sesia-Lanzo zone, Western Alps). Rendiconti della Società Italiana di Mineralogia e Petrologia, 33: 389-407.

Hobbs, B.E., Means, W.D. and Williams, P.F. (1976). An outline of structural geology. Wiley, New York, 571 pp.

Hobbs, B.E., Ord, A., Spalla, M.I., Gosso, G. and Zucali, M. (2010). The interaction of deformation and metamorphic reactions. Geological Society of London Special Publication, 332: 189-222. 10.1144/SP332.12

Holland, T.J.B. and Powell, R. (1998). An internally-consistent thermodynamic data set forphases of petrological interest. Journal of Metamorphic Geology, 16: 309-343. 10.1111/j. 1525-1314.1998.00140.x

Hy, C. (1984). Métamorphisme polyphasé et évolution tectonique dans la croûte continentale éclogitisée: les séries granitiques et pélitiques du Monte Mucrone (zone Sesia-Lanzo, Alpes italiennes). PhD Thesis, Université Paris VI, 198 pp.

Johnson, S.E. and Vernon, R.H. (1995). Inferring the timing of porphyroblast growth in the absence of continuity between inclusion trails and matrix foliations: can it reliably done? Journal of Structural Geology, 17(8): 1203-1206. 10.1016/0191-8141(95)00021-5

Koons, P.O., Rubie, D.C. and Frueh-Green, G. (1987). The effects of disequilibrium and deformation on the mineralogical evolution of quartz-diorite during metamorphism in the eclogite facies. Journal of Petrology, 28: 679-700. 10.1093/petrology/28.4.679

Krogh Ravna, E. (2000). The garnet-clinopyroxene Fe2+-Mg geothermometer: an updated calibration. Journal of Metamorphic Geology, 18(2): 211-219. 10.1046/j. 1525-1314.2000.00247.x

Laird, J. and Albee, A.L. (1981). Pressure, temperature and time indicators in mafic schists: their application to reconstructing the polymetamorphic history of Vermont. American Journal of Science, 281: 127-175. 10.2475/ajs. 281.2.127

Lardeaux, J.M., 1981. Evolution tectono-metamorphique de la zone nord du Massif de Sesia-Lanzo (Alpes occidentales): un exemple d'éclogitisation de croute continentale. PhD Thesis, Université Paris VI, 226 pp.

Lardeaux, J.M., Gosso, G., Kienast, J.R. and Lombardo, B. (1982). Relations entre le métamorphisme et la déformation dans la zone Sésia-Lanzo (Alpes Occidentales) et le problème de l'éclogitisation de la croûte continentale. Bulletin de la societé géologique de France, 24: 793-800.

Lardeaux, J.M., Gosso, G., Kienast, J.R. and Lombardo, B. (1983). Chemical variations in phengitic micas of successive foliations within the Eclogitic Micaschists complex, Sesia-Lanzo zone (Italy, Western Alps). Bulletin de Minéralogie, 106: 673-689.

Lardeaux, J.M. and Spalla, M.I. (1991). From granulites to eclogites in the Sesia zone (Italian Western Alps): a record of the opening and closure of the Piedmont ocean. Journal of Metamorphic Geology, 9: 35-59. 10.1111/j. 1525-1314.1991.tb00503.x

Liu, J., Bohlen, S.R. and Ernst, W.G. (1996). Stability of hydrous phases in subducting oceanic crust. Earth and Planetary Science Letters, 143: 161-171. 10.1016/0012-821X(96)00130-6

Maffeo, B., 1970. Studio petrografico dell'ammasso granitico del Monte Mucrone e dei suoi rapporti con i «micascisti eclogitici». Unpublished Tesi di Laurea, Università di Torino, 117 pp.

Marotta, A.M. and Spalla, M.I. (2007). Permian-Triassic high thermal regime in the Alps: result of Late Variscan collapse or continental rifting? Validation by numerical modeling. Tectonics, 26: TC4016, 10.1029/2006TC002047

Marotta, A.M., Spalla, M.I. and Gosso, G. (2009). Upper and lower crustal evolution during lithospheric extension: numerical modelling and natural footprints from the European Alps. Geological Society of London Special Publication, 321: 33-72. 10.1144/SP321.3

Massonne, H.J. and Schreyer, W. (1987). Phengite geobarometry based on the limiting assemblage with k-feldspar, phlogopite and quartz. Contributions to Mineralogy and Petrology, 96: 212-224. 10.1007/BF00375235

Meda, M., Marotta, A.M. and Spalla, M.I. (2010). The role of mantle hydration into continental crust recycling in the wedge region. Geological Society of London Special Publication, 332: 149-172. 10.1144/SP332.10

Moody, J.B., Meyer, D. and Jenkins, J.E. (1983). Experimantal characterization of the greenschist-amphibolite boundary in mafic system. American Journal of Science, 283: 48-92. 10.2475/ajs.283.1.48

Morimoto, N. (1988). Nomenclature of pyroxenes. Mineralogical Magazine, 52: 535-550. 10.1180/minmag. 1988.052.367.15

Oberhaensli, R., Hunziker, J.C., Martinotti, G. and Stern, W.B. (1985). Geochemistry, gheochronology and Petrology of Monte Mucrone: an example of Eo-Alpine eclogitisation of Permian granitoids in the Sesia-Lanzo Zone, Western Alps, Italy. Chemical Geology, 52: 165-184.

Park, R.G. (1969). Structural correlations in metamorphic belts. Tectonophysics, 7(4): 323-338. 10.1016/0040-1951(69)90077-8

Passchier, C.W., Myers, J.S. and Kröner, A. (1990). Field geology of high-grade gneiss terrains. Springer Verlag, Berlin, 150 pp. 10.1007/978-3-642-76013-6

Passchier, C.W. and Trouw, R.A.J. (2005). Microtectonics, Second Edition. Springer, 366 pp.

Plyusnina, L.P. (1982). Geothermometry and geobarometry of plagiocalse-hornblende bearing assemblages. Contributions to Mineralogy and Petrology, 80: 140-146. 10.1007/BF00374891

Pognante, U. (1989a). Lawsonite, blueschist and eclogite formation in the southern Sesia Zone (Western Alps, Italy). European Journal of Mineralogy, 1: 89-104.

Pognante, U. (1989b). Tectonic implications of lawsonite formation in the Sesia zone (Western Alps). Tectonophys., 162: 219-227. 10.1016/0040-1951(89)90245-X

Pognante, U. (1991). Petrological constraints on the eclogite- and blueschist-facies metamorphism and P-T-t paths in the Western Alps. Journal of Metamorphic Geology, 9: 5-17. 10.1111/j.1525-1314.1991.tb00501.x

Poli, S. (1993). The amphibolite-eclogite transformation: an experimental study on basalt. American Journal of Science, 293: 1061-1107. 10.2475/ajs.293.10.1061

Poli, S. and Schmidt, M.W. (1995). H2O transport and release in subduction zones: experimental constraints on basaltic and andesitic system. Journal of Geophisical Research, 100(B11): 22299 - 22314. 10.1029/95JB01570

Powell, R. and Holland, T.J.B. (1994). Optimal geothermometry and geobarometry. American Mineralogist, 79: 120-133.

Ramsay, J.G., 1967. Folding and Fracturing of Rocks. McGraw-Hill, New York, 568 pp.

Rebay, G. and Messiga, B. (2007). Prograde metamorphic evolution and development of chloritoid-bearing eclogitic assemblages in subcontinental metagabbro (Sesia-Lanzo Zone, Italy). Lithos, 98: 275-291. 10.1016/j.lithos. 2007.04.002

Rebay, G. and Spalla, M.I. (2001). Emplacement at granulite facies conditions of the Sesia-Lanzo metagabbros: an early record of Permian rifting? Lithos, 58: 85-104. 10.1016/S0024-4937(01)00046-9

Roda, M., Spalla, M.I. and Marotta, A.M. (2012). Integration of natural data within a numerical model of ablative subduction: a possible interpretation for the Alpine dynamics of the Austroalpine crust. Journal of Metamorphic Geology, 30: 973-996. 10.1111/jmg.12000

Roda, M. and Zucali, M. (2008). Meso and microstructural evolution of the Mont Morion metaintrusive complex (Dent-Blanche nappe, Austroalpine domain, Valpelline, Western Italian Alps). Bollettino della Società Geologica Italiana, 127, 1-19.

Roda, M. and Zucali, M. (2011). Tectono-metamorphic map of the Mont Morion Permian metaintrusives (Mont Morion - Mount Collon - Matterhorn Complex, Dent Blanche Unit), Valpelline -Western Italian Alps. Journal of Maps, 2011: 519-535.

Rubatto, D., Gebauer, D. and Compagnoni, R. (1999). Dating of eclogite-facies zircons; the age of Alpine metamorphism in Sesia-Lanzo Zone (Western Alps). Earth and Planetary Science Letters, 167: 141-158. 10.1016/S0012-821X(99)00031-X

Salvi, F., Spalla, M.I., Zucali, M. and Gosso, G. (2010). Three-dimensional evaluation of fabric evolution and metamorphic reaction progress in polycyclic and polymetamorphic terrains: a case from the Central Italian Alps. Geological Society of London Special Publication, 332: 173-187. 10.1144/SP332.11

Schmidt, M.W. (1993). Phase relations and compositions in tonalite as a function of pressure: an experimental study at 650°C. American Journal of Science, 293: 1011-1060. 10.2475/ajs.293.10.1011

Spalla, M.I. (1983). Struttura e petrografia delle successioni del margine esterno della zona Sesia-Lanzo al contatto con la Falda Piemontese tra il lago di Monastero e il Ponte Cusard (Valli di Lanzo). Unpublished Tesi di Laurea, Università di Torino, 181 pp.

Spalla, M.I. (1993). Microstructural control on the P-T path construction in the metapelites from the Austroalpine crust (Texel Gruppe, Eastern Alps). Schweizerische Mineralogische und Petrographische Mitteilungen, 73: 259-275.

Spalla, M.I., De Maria, L., Gosso, G., Miletto, M. and Pognante, U. (1983). Deformazione e metamorfismo della Zona Sesia - Lanzo meridionale al contatto con la falda piemontese e con il massiccio di Lanzo, Alpi occidentali. Memorie della Società Geologica Italiana, 26: 499-514.

Spalla, M.I., Lardeaux, J.M., Dal Piaz, G.V. and Gosso, G. (1991). Metamorphisme et tectonique a la marge externe de la zone Sesia-Lanzo (Alpes occidentales). Memorie di Scienze Geologiche, Padova, 43: 361-369.

Spalla, M.I., Siletto, G.B., di Paola, S. and Gosso, G. (2000). The role of structural and metamorphic memory in the distinction of tectono-metamorphic units: the basement of the Como Lake in the Southern Alps. Journal of Geodynamics, 30: 191-204. 10.1016/S0264-3707(99)00033-2

Spalla, M.I., Zanoni, D., Williams, P. and Gosso, G. (2011). Deciphering cryptic P-T-d-t histories in the western Thor-Odin dome, Monashee Mountains, Canadian Cordillera: A key to unravelling pre-Cordilleran tectonic signatures. Journal of Structural Geology, 33: 399-421. 10.1016/j.jsg. 2010.11.014

Spalla, M.I. and Zucali, M. (2004). Deformation vs. metamorphic re-equilibration heterogeneities in polymetamorphic rocks: a key to infer quality P-T-d-t path. Periodico di Mineralogia, 73(2): 249-257.

Spalla, M.I., Zucali, M., di Paola, S. and Gosso, G. (2005). A critical assessment of the tectono-thermal memory of rocks and definition of tectono-metamorphic units: evidence from fabric and degree of metamorphic transformations. Geological Society of London Special Publication, 243: 227-247 pp.

Turner, F.J. and Weiss, L.E. (1963). Structural analysis of metamorphic tectonites. MacGraw-Hill, New York, 545 pp.

Ungaretti, L., Lombardo, B., Domeneghetti, C. and Rossi, G. (1983). Crystal-chemical evolution of amphiboles from eclogitized rocks of the Sesia-Lanzo Zone, Italian western Alps. Bulletin de Minéralogie, 106: 645-672.

Whitney, D.L. and Evans, B.W. (2010). Abbreviations for names of rock-forming minerals. American Mineralogist, 95: 185-187. 10.2138/am.2010.3371

Williams, P.F. (1985). Multiply deformed terrains - problems of correlation. Journal of Structural Geology, 7(3/4): 269-280. 10.1016/0191-8141(85)90035-5

Wu, C.M., Wang, X.S., Yang, C.H., Geng, Y.S. and Liu, F.L. (2002). Empirical garnet-muscovite geothermometry in metapelites. Lithos, 62: 1-13. 10.1016/S0024-4937(02)00096-8

Zanoni, D. (2010). Structural and petrographic analysis at the north-eastern margin of the Oligocene Traversella pluton (Internal Western Alps, Italy). Italian Journal of Geosciences, 129(1): 51-68.

Zanoni, D., Bado, L. and Spalla, M.I. (2008). Structural analysis of the Northeastern margin of the Tertiary intrusive stock of Biella (Western Alps, Italy). Bollettino della Società Geologica Italiana, 127(1): 125-140.

Zanoni, D., Spalla, M.I. and Gosso, G. (2010). Structure and PT estimates across late-collisional plutons: constraints on the exhumation of Western Alpine continental HP units. International Geology Review, 52: 1244-1267. 10.1080/00206814.2010.482357

Zucali, M. (2002). Foliation map of the "Eclogitic Micaschists Complex" (M. Mucrone-M.Mars-Mombarone, Sesia-Lanzo Zone, Italy). Memorie di Scienze Geologiche, Padova, 54: 87-100.

Zucali, M., Chateigner, D., Dugnani, M., Lutterotti, L. and Ouladdiaf, B. (2002a). Quantitative texture analysis of naturally deformed hornblendite under eclogite facies conditions (Sesia-Lanzo Zone, Western Alps): comparison between x-ray and neutron diffraction analysis. Geological Society of London Special Publication, 200: 239-253. 10.1144/GSL.SP.2001.200.01.14

Zucali, M. and Spalla, M.I. (2011). Prograde lawsonite during the flow of continental crust in the Alpine subduction: Strain vs. metamorphism partitioning, a field-analysis approach to infer tectonometamorphic evolutions (Sesia-Lanzo Zone, Western Italian Alps). Journal of Structural Geology, 33: 381-398. 10.1016/j.jsg.2010.12.006

Zucali, M., Spalla, M.I. and Gosso, G. (2002b). Fabric evolution and reaction rate as correlation tool: the example of the Eclogitic Micaschists complex in the Sesia-Lanzo Zone (Monte Mucrone – Monte Mars, Western Alps Italy). Schweizerische Mineralogische und Petrographische Mitteilungen, 82: 429-454.

Zucali, M. 2011. Coronitic microstructures in patchy eclogitised continental crust: the Lago della Vecchia pre-Alpine metagranite (Sesia-Lanzo Zone, Western Italian Alps). In: (Ed.) M.A. Forster, and J.D. Fitz Gerald, The Science of Microstructure - Part II, Journal of the Virtual Explorer, Electronic Edition, ISSN 1441-8142, volume 38, paper 5, 10.3809/jvirtex.2011.00286